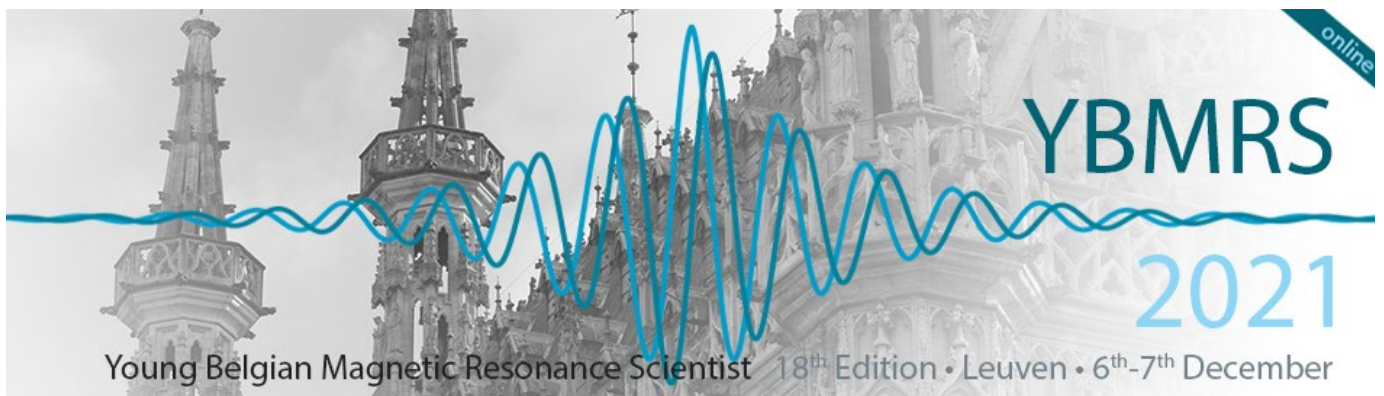


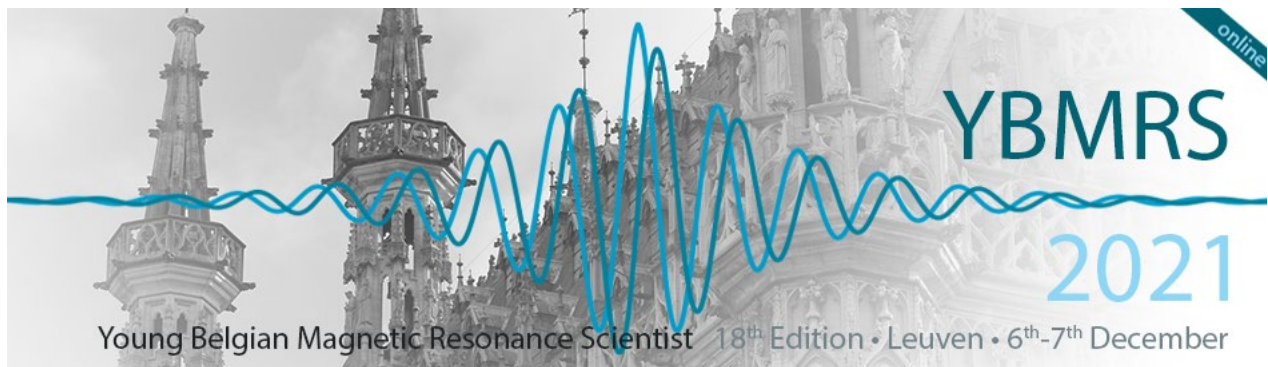
# Young Belgian Magnetic Resonance Scientist Symposium

18<sup>th</sup> Edition



**December 6-7, 2021**  
**Leuven, Belgium**





# PROGRAM & ABSTRACTS

## ORGANIZING COMMITTEE

Dimitrios Sakellariou, KU Leuven  
Wim De Borggraeve, KU Leuven  
Tatjana Vogt, KU Leuven  
Annelies Vanvlasselaer, KU Leuven  
Gert Steurs, KU Leuven

## SCIENTIFIC COMMITTEE

Peter Adriaensens, UHasselt  
Carmela Aprile, UNamur  
Gilles Bruylants, ULB  
Christian Damblon, ULiège  
Luca Fusaro, UNamur  
Bernard Gallez, UC Louvain  
Céline Henoumont, UMONS  
Uwe Himmelreich, KU Leuven  
José Martins, UGent  
Dimitrios Sakellariou, KU Leuven  
Sabine Van Doorslaer, UAntwerpen



**The Organizing Committee gratefully  
acknowledges the following institutions,  
societies and companies for their kind support:**

Platinum Sponsor



Gold Sponsor



Academic and non-profit institutions



Dear Magnetic Resonance Scientists,

Many things have changed in the way scientific meetings take place. Our motivation to keep this event active for the community remains very strong in these special times. It has been long but the YBMRS symposium is echoing back in KU Leuven!

In the spirit of the previous editions, the aim of the symposium is to give young researchers the opportunity to present their latest work, to promote discussions and exchange ideas around different areas using magnetic resonance and nurture possible new collaborations.

This year the symposium will be held online and last two days, with oral presentations, one educational talk, four plenary talks and opportunities to interact with everyone active in magnetic resonance in Belgium, be it in research and/or in industry.

This edition will be held on **Monday 6th and Tuesday 7th of December 2021**.

We hope to "see" you all there!

The organizing committee,  
Dimitrios Sakellariou, Tatjana Vogt and Wim De Borggraeve

## PROGRAM

Monday December 6<sup>th</sup> 2021

- 08:30 **Welcome and opening** by the Organizing Committee
- Plenary session 1**  
*Chair: Prof. Dimitrios Sakellariou (KU Leuven)*
- 08:40 **ED1: Solid-state NMR**  
Prof. Lyndon Emsley (École Polytechnique Fédérale de Lausanne)
- 09:35 Short break
- Plenary session 2**  
*Chair: Prof. Luca Fusaro (Université de Namur)*
- 10:00 **OC1: Dual EPR measurement of oxygen consumption and superoxide production: principle and applications** p. 25  
*Donatienne d'Hose (UCLouvain)*
- 10:20 **OC2: Development and characterization of paramagnetic bimodal contrast agents for paraCEST and <sup>19</sup>F MRI** p. 26  
*Pierre Ernotte (UMons)*
- 10:40 **OC3: Surface grafting of aminopropylphosphonic acid on titania powder: the role of the amine functionality on the surface interaction and coordination** p. 27  
*Nick Gys (VITO)*
- 11:00 **OC4: Low field and high field NMR response on Fe<sup>3+</sup> loaded inorganic polymers** p. 28  
*Ziyou Yu (KU Leuven)*
- 11:20 Short break
- Plenary session 3**  
*Chair: Prof. Sabine Van Doorslaer (Universiteit Antwerpen)*
- 11:45 **PL1: High field EPR and DNP** p. 11  
Prof. Thomas Prisner (Goethe University Frankfurt)
- 12:35 Lunch break
- Poster session**  
*Chair: Prof. Wim De Borggraeve (KU Leuven)*
- 14:00 **Flash presentations of posters**
- 14:25 **Poster session**
- 16:10 Short break
- Plenary session 4**  
*Chair: Prof. Luca Fusaro (Université de Namur)*
- 16:25 **PL2: NMR crystallography** p. 13  
Prof. Lyndon Emsley (École Polytechnique Fédérale de Lausanne)
- 17:15 **PI meeting**
- 17:50 **Discussion news from the MR community in Belgium**

## PROGRAM

Tuesday December 7<sup>th</sup> 2021

- 08:30 **Welcome** by the Organizing Committee
- Plenary session 5**  
*Chair: Prof. Gilles Bruylants (ULB)*
- 08:35 **PL3: Opportunities offered by ultra-high field MRI** p. 15  
Dr. Luisa Ciobanu (CEA Saclay)
- 09:25 **SP1: Fast multinuclear benchtop NMR spectroscopy – how the highest sensitivity saves you time and enables new applications** p. 21  
Presentation by Dr. H el ene Freichels (Magritek)
- 09:45 Short break
- Plenary session 6**  
*Chair: Prof. Peter Adriaensens (UHasselt)*
- 10:15 **OC5: Characterization of tumor heterogeneity using multi-parametric MRI and unsupervised classification methods** p. 29  
*Matic Pusovnik (KU Leuven)*
- 10:35 **OC6: Rapid structural elucidation of cyclic lipopeptides via NMR fingerprint matching** p. 30  
*Dr. Niels Geudens (UGent)*
- 10:55 **OC7: Additive manufacturing for the fabrication of subject-specific MRI passive shim and RF coil configurations** p. 31  
*Hanne Vanduffel (KU Leuven)*
- 11:15 Lunch break
- Plenary session 7**  
*Chair: Chair: Prof. Christian Dambon (Universit e de Li ege)*
- 13:00 **PL4: The NMR Contribution to Cellular Structural Biology** p. 17  
Prof. Lucia Banci (University of Florence)
- 15:20 **OC8: A unique quantitative <sup>1</sup>H-NMR approach for lung cancer detection using a plasma protein-binding competitor** p. 32  
*Elien Derveaux (UHasselt)*
- 15:40 **OC9: Pitfalls in sample preparation of metalloproteins for low-temperature EPR: the example of alkaline myoglobin** p. 33  
*Ilenia Serra (UAntwerp)*
- 16:00 **OC10: NMR as a versatile tool to investigate supramolecular hydrogelation** p. 34  
*Ruben Van Lommel (KU Leuven)*
- 14:50 Break / **Decision on prizes**
- 15:30 **Awards session & closing ceremony**



## LIST OF POSTERS

- P1 Low resolution nuclear magnetic resonance for the study of nickel (II) and manganese (II) removal by ion exchange resin** p. 37  
M. Bernardi
- P2 Impact of inhibition of the mitochondrial pyruvate carrier on the tumor extracellular pH as measured by CEST-MRI** p. 38  
C. Buyse, N. Joudiou, C. Corbet, O. Feron, L. Mignon, J. Flament, B. Gallez
- P3 The use of cerebral perfusion MRI in a rat model to investigate the key role of microvascular rarefaction in the development of Vascular Cognitive Impairment** p. 39  
B. Callewaert, W. Gsell, E. A. V. Jones and U. Himmelreich
- P4 NMR studies of hydrogen-bonded water-aminium assemblies templating SAPO materials** p. 40  
C.V. Chandran, S. Radhakrishnan, S. H. Park, W. Choi, K. C. Kemp, R. G. Bell, C. E. A. Kirschhock, S. B. Hong, E. Breynaert
- P5 Relaxorption: a new in situ NMR measurement for adsorption** p. 41  
R. de Oliveira Silva, J. Marreiros, R. Ameloot, D. Sakellariou
- P6 Engineering microbial cells for the biosynthesis of novel anticancer agents** p. 42  
D. De Ruyscher, E. Vriens, G. Steurs, W. De Borggraeve and J. Masschelein
- P7 <sup>13</sup>C-MRS metabolic markers of response to targeted therapies in YUMM 1.7 melanoma xenografts** p. 43  
C. Farah, L. Mignon, M.A. Neveu , C. Bouzin , F. Gourgue , N. Joudiou , C. Yelek , J.F. Baurain , B. Jordan
- P8 New Platforms Dedicated to MRI/PAI Bimodal Imaging: Molecular and Nanoparticulate Approaches** p. 44  
C. Gosée, C. Cadiou, J. Moreau, M. Callewaert, L. Larbanoix, F. Chuburu, S. Laurent
- P9 Development of a combined methodology towards mechanistic investigation of rare metal-free, light activated catalysts** p. 45  
A. Guidetti, K. Gadde, H.Y.V. Ching, G. Mitrikas, B.U.W. Maes, S. Van Doorslaer
- P10 Petrophysical characterization and shale-gas potential of the Late Paleocene Patala Formation, Potwar Basin, Pakistan (Eastern Tethys): Comparative study on porosity distribution in mudstones** p. 46  
N. Khan, H. Claes, R. de Oliveira-Silva, G.J. Weltje, R. Swennen
- P11 Simulation of Nuclear Magnetic Relaxation Induced by Superparamagnetic Nanoparticles trapped in a biological tissue** p. 47  
E. Martin, Y. Gossuin, Q.L. Vuong
- P12 Trace level detection and quantification of crystalline silica in an amorphous silica matrix with natural abundance <sup>29</sup>Si NMR** p. 48  
S. Radhakrishnan, H. Colaux, C. Vinod Chandran, D. Dom, L. Verheyden, F. Taulelle, J. A. Martens, and E. Breynaert
- P13 NMR crystallography reveals carbonate induced Al-ordering in ZnAl layered double hydroxide** p. 49  
S. Radhakrishnan, K. Lauwers, C. Vinod Chandran, J. Trébosc, S. P. Sree, J. A. Martens, F. Taulelle, C. E. A. Kirschhock and E. Breynaert

- P14 The impact of macrocycle formation on the conformation of tolaasin I as revealed by NMR spectroscopy** p. 50  
D. Roelandt, B. Kovács, N. Geudens, J.C. Martins
- P15 The non-innocent role of spin-traps in monitoring radical formation in copper-catalyzed reactions** p. 51  
M. Samanipour, H. Y. V. Ching, H. Streckx, B. U. W. Maes, S. Van Doorslaer
- P16 Towards a better understanding of the underlying molecular mechanisms during an aptamer-target interaction, an NMR analysis of TESS.1** p. 52  
S. Schellinck, D. Buyst, A.M. de Vries, E. Daems, R. Cánovas, K. De Wael, A. Madder, J.C. Martins
- P17 Characterization of microbial degradation products of steviol glycosides** p. 53  
G. Steurs, N. Moons, L. Van Meervelt, B. Meesschaert and W.M. De Borggraeve
- P18 Isotopological Fingerprinting Enables Conformational Analysis of Hydrogenation Catalysts** p. 54  
E. Vaneckhaute, J.M. Tyburn, J.G. Kempf, J.A. Martens, E. Breynaert
- P19 Quantification of 2-disulfide bonded isomers of apamin, a peptidic toxin, leads to the observation of a structural rearrangement** p. 55  
M. Wanko, J.L. Hayen, R. Vitello, C.Damblon, J.F. Liégeois

## Plenary Lectures



## PL1

### **High field EPR and DNP**

Prof. Thomas Prisner

*Goethe University Frankfurt, Germany*

High-field EPR spectroscopy spectrally resolves the g-tensor anisotropy of organic radicals in frozen solutions. This allows to perform orientation selective pulse-EPR by selecting specific molecular orientations with respect to the external magnetic field in disordered frozen powder samples. I will show applications to pulsed dipolar EPR spectroscopy (PDS) on nucleic acid molecules with cytidine analogous spin labels, allowing to obtain very precise distances and to obtain additional angular restraints, which help to better describe the conformation of the oligonucleotide with few spin label pairs. A challenge at high magnetic fields is the lower available microwave power, which does not allow to excite or to saturate the whole EPR line. Shaped microwave pulses can be used to enlarge the excitation bandwidth and improve PDS experiments. Double resonance structures for electron spin (260 GHz) and proton nuclear spins (400 MHz) can be used for electron nuclear double resonance (ENDOR) experiments or – vice versa – for dynamic nuclear polarization (DNP). New experimental results on viscous liquids at ambient temperatures will be shown and discussed.



**PL2**

**NMR crystallography**

Prof. Lyndon Emsley

*École Polytechnique Fédérale de Lausanne, France*





## PL3

### **Opportunities offered by ultra-high field MRI**

Dr. Luisa Ciobanu

*CEA Saclay*

The intent of this presentation is to discuss the main advantages of imaging at ultra-high magnetic field (UHF). As low sensitivity is the most common drawback of MRI applications, the most obvious opportunity of UHF is the increased sensitivity, reflected in higher Signal-to-Noise ratio (SNR). This SNR increase can be used for faster imaging and/or higher spatial resolution. In addition, UHF offers enhanced magnetic susceptibility contrast, which enables high-resolution functional MRI studies allowing detailed characterization of neuronal activity in specific brain structures. Besides high resolution anatomical and functional MRI, UHF is also advantageous for other applications including metabolic imaging and non-proton (X-nuclei) imaging.



## PL4

### **The NMR Contribution to Cellular Structural Biology Abstract**

Prof. Lucia Banci

*University of Florence, Italy*

NMR spectroscopy can provide unique contributions for the description of cellular processes, as it is indeed suitable not only for characterizing the structural and dynamical properties of biomolecules but, even more importantly, for describing transient interactions and functional events with atomic resolution possibly in a cellular context. This requires the development of suitable methodologies capable of addressing multiple, specific, and sometimes non-conventional aspects for describing functional processes in cells.

In-cell NMR, i.e. the collection of high resolution NMR spectra of biomolecules in intact, living cells, represents one of the highest impact applications of magnetic resonance.

These experiments allow us to obtain information on the conformational and functional properties of biomolecules at atomic resolution in conditions as close as possible to the physiological ones. In cell NMR also allows to monitor protein-protein interactions and to follow functional processes in real time as well as to perform drug screening at cellular level.

NMR is also essential for optimization of biological drugs and of vaccines. Furthermore the availability of Ultra High Magnetic fields allows the analysis of biological drugs without the need of isotope labelling.



## Sponsor Presentation



## SP1

### **Fast multinuclear benchtop NMR spectroscopy – how the highest sensitivity saves you time and enables new applications**

Dr. H el ene Freichels

*Magritek*

The sensitivity and resolution of Benchtop NMR spectrometers has been steadily improving over the last years as more and more powerful magnets and electronics are made available. With the launching of the Spinsolve 90, Magritek has taken another step towards achieving higher resolution and sensitivity on the bench. These powerful magnets are now available with automatic multinuclear probes which makes it possible to measure multiple nuclei on the same instrument (Spinsolve Multi X).

As the performance and capability of benchtop NMR spectrometers increase, so does the range of applications that the instrument can address. This presentation will describe the latest benchtop NMR applications and show extensive example NMR data highlighting the ever-increasing potential of these systems. The Spinsolve 90 has high sensitivity that enables advanced experiments, such as HSQC-ME, to be acquired in just 2 minutes. Modern techniques such as NUS can make experiments even quicker reducing the time chemists have to wait for NMR results. The versatility of the Spinsolve Multi X probes, which can automatically switch between several X-nuclei like  $^{13}\text{C}$ ,  $^{31}\text{P}$ ,  $^7\text{Li}$ ,  $^{29}\text{Si}$ , (among others) enabling advanced multinuclear measurements to be made without operator intervention will be shown.





## Oral Communications



## Dual EPR measurement of oxygen consumption and superoxide production: Principle and applications

D. d'Hose<sup>1</sup>, L. Mignon<sup>1</sup>, P. Danhier<sup>1</sup>, P. Isenborghs<sup>1</sup>, H. Northshield<sup>1</sup>, B.F. Jordan<sup>1</sup> and B. Gallez<sup>1</sup>

<sup>1</sup> Biomedical Magnetic Resonance, Louvain Drug Research Institute (LDRI), Université Catholique de Louvain (UCLouvain), Brussels, Belgium

A growing body of evidence indicates that mitochondria play a key role in many disorders as well as in cancer progression and response to treatment. Next to being the main cellular energy generator through respiration, mitochondria are also the major producer of superoxide and other downstream reactive oxygen species (ROS) in the cell. Over the years, several mitochondrial modulators have emerged, notably in the field of anticancer therapies targeting cellular oxygenation and mitochondrial metabolism. Their impact on the oxygen consumption rate (OCR) and bioenergetics of this organelle is nowadays well studied but little has been investigated on their potential underlying incidence on reactive oxygen species (ROS) production and oxidative damage occurring during those treatments. When the balance between antioxidant systems and cellular ROS is disrupted, oxidative stress overpowers and leads to the oxidation of macromolecules like DNA, proteins and lipids, consequently inducing cellular damage and defects in cell signalling. More specifically, superoxide may trigger cell death when produced in large excess. Potential toxic agents acting on the mitochondrial electron transport chain (ETC) could therefore be harmful for human health (or even eukaryotes in general). On the other hand, several drugs were shown to inhibit the oxygen consumption rate (OCR) in tumors, subsequently enhancing the efficacy of radiation therapy by increasing tumor pO<sub>2</sub> and potentially leading to decreased tumor volume via superoxide-induced cell death. However, when produced at a more moderate level, superoxide was suggested to be a key driver promoting cancer cell migration and metastasis. Therefore, these dual dose-dependent effects are important to study when considering the effect of a drug as a potential radiosensitizer in radiation therapy, but also to evaluate the potential toxicity of diverse agents before being placed on the market. So far, no technology was able to assess simultaneously the consumption of oxygen and the leakage of superoxide from the electron transport chain in a sensitive and specific manner compared to currently used tools.

Recently, our lab developed an integrated toolbox enabling the simultaneous analysis of the OCR and superoxide production on a single mitochondrial preparation [1]. EPR spectroscopy allows the measurement of both components either independently or simultaneously in a same cellular or mitochondrial preparation. OCR determination using EPR oximetry is based on the change in EPR linewidth of a paramagnetic oxygen sensing probe (a perdeuterated nitroxide) in the presence of oxygen consuming cells in a closed system. Superoxide production can be monitored by the oxidation of cyclic hydroxylamines into nitroxides. The contribution of superoxide to the nitroxide formation is deduced from experiments in the presence and in the absence of SOD and PEGSOD as appropriate controls. This EPR toolbox was used to assess mitochondrial dysfunction on human cells after SDHI fungicide treatment [2] and to evaluate statins' ability to radiosensitize prostate cancer cells.

1. d'Hose, D., Danhier, P., *et al.*, *Redox biol.* 2021, **40**, 101852.
2. d'Hose, D., Isenborghs, P., *et al.*, *Molecules* 2021.

## Development and characterization of paramagnetic bimodal contrast agents for paraCEST and $^{19}\text{F}$ MRI

Pierre Ernotte<sup>[a]</sup>, Céline Henoumont<sup>[a]</sup>, Sébastien Boutry<sup>[b]</sup>, Sophie Laurent<sup>[a], [b]</sup>

[a] General, Organic and Biomedical Chemistry, NMR and Molecular Imaging laboratory, University of Mons, 7000 Mons (Belgium)

[b] Center for Microscopy and Molecular Imaging (CMMI), 6041 Charleroi-Gosselies (Belgium)

Magnetic Resonance Imaging (MRI) is a widely used imaging technique and often requires the use of contrast agents to increase its sensitivity. Several classes of contrast agents are under development, as paraCEST or  $^{19}\text{F}$  MRI contrast agents. In this work, bimodal agents active in both paraCEST and fluorine MRI are synthesized by adding fluorine atoms to the paraCEST complexes. The interaction between fluorine atoms and paramagnetic ions can generate an increase in  $^{19}\text{F}$  MRI sensitivity by decreasing  $^{19}\text{F}$  relaxation times.

DOTAM derivatives, fully synthesized using cyclen as starting material, were chosen as paraCEST ligands because they are well known to reduce the innersphere water exchange rate, generating a strong CEST effect. Bis-trifluoro benzylamine was then grafted to the chelates using a lysine derivative.

The ligands were characterized by NMR and ESI-MS and were finally complexed with thulium, ytterbium and europium. To characterize the CEST efficiency, Z-spectra were recorded using a 679Hz saturation pulse, at 37°C and 600MHz. To evaluate the  $^{19}\text{F}$  MRI efficiency,  $^{19}\text{F}$  relaxation time measurements were performed at 11.75 Tesla.

The europium complex shows an expected great CEST signal at around 50ppm, which is due to one coordinated innersphere water molecule. Thulium and ytterbium complexes demonstrate two CEST signals, probably due to the two types of amides present on the chelate. Measurements of  $^{19}\text{F}$  relaxation times were then performed before and after complexation to highlight the influence of the paramagnetic ion on those relaxation times. It was observed that europium has a weak impact whereas ytterbium, and more specifically thulium has a greater influence.

In conclusion, the complexes were successfully synthesized and characterized. The europium bimodal complex exhibits a great CEST effect but has relatively long  $^{19}\text{F}$  relaxation times. The thulium and the ytterbium complexes both have a lower CEST effect, but they reduce the  $^{19}\text{F}$  relaxation times more efficiently. To increase their sensitivity, the grafting on a nanoplatfrom is being studied.

## Surface grafting of aminopropylphosphonic acid on titania powder: the role of the amine functionality on the surface interaction and coordination

N. Gys<sup>1,2</sup>, L. Siemons<sup>3</sup>, B. Pawlak<sup>4</sup>, K. Wyns<sup>1</sup>, K. Baert<sup>5</sup>, T. Hauffman<sup>5</sup>, P. Adriaensens<sup>4</sup>, F. Blockhuys<sup>3</sup>, B. Michielsen<sup>1</sup>, S. Mullens<sup>1</sup> and V. Meynen<sup>1,2</sup>

<sup>1</sup> Sustainable Materials, Flemish Institute for Technological Research (VITO NV), Mol

<sup>2</sup> Laboratory of Adsorption and Catalysis (LADCA), University of Antwerp, Wilrijk

<sup>3</sup> Structural Chemistry Group, University of Antwerp, Antwerp

<sup>4</sup> Analytical and Circular Chemistry (ACC), University of Hasselt, Diepenbeek

<sup>5</sup> Research Group Electrochemical and Surface Engineering (SURF), Vrije Universiteit Brussel, Brussels

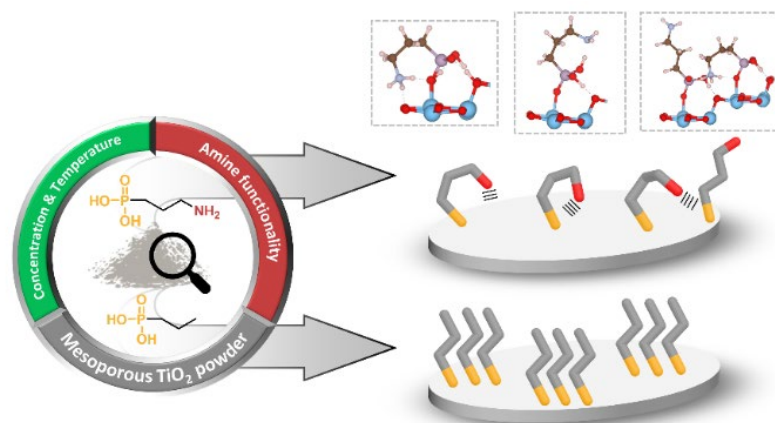
Surface modification (grafting) of metal oxides with organophosphonic acids bearing terminal amine functionalities is of high relevance to extend the functionality and applicability of these materials.<sup>1,2</sup> However, previous studies focus primarily on the application perspective while a systematic characterization of the modified surface and further insights and evidence of specific conformations of grafted amine-bearing groups at the molecular level are missing.

In this work<sup>3</sup>, TiO<sub>2</sub> powder is grafted with 3-aminopropylphosphonic acid at different concentrations (20, 75, 150 mM) and temperatures (50, 90 °C) and compared with propylphosphonic acid grafting to elucidate the impact of the amine group on the surface properties. These are characterized via a combination of complementary spectroscopic techniques, including DRIFT, XPS and solid-state <sup>31</sup>P MAS NMR. This is supported by Density Functional Theory-Periodic Boundary Conditions (DFT/PBC) calculations on clean and hydrated surfaces, to gain insights into the different surface conformations based on calculated adsorption energies and calculated <sup>31</sup>P chemical shifts that are correlated to the experimental spectra.

Both the experimental and computational work reveal a coexistence of a variety of surface conformations, wherein the amine groups are involved in inter- and intra-adsorbate (i.e. 3APPA) and adsorbate-surface interactions. On a fully hydrated surface, most strongly resembling experimental conditions, differences in adsorption energies between the conformations are too small to make conclusive statements on their prevalence nor in their relative order of occurrence. This is in agreement with the calculated <sup>31</sup>P chemical shifts associated with each conformation, which strongly overlap with the broad band found in the experimental spectra.

This coexistence of multiple interaction sites of the amine group might have consequences on their behavior in applications, since the accessibility of the amine groups for adsorption of molecules or subsequent conjugation reactions might be hindered or altered. Since material synthesis and application are highly correlated, the results of this work provide a better understanding towards the use and performance of amine-containing organophosphonic acid modified TiO<sub>2</sub> materials.

1. Queffelec, C., Petit, M., Janvier, P., Knight, D. A. & Bujoli, B. *Chem. Rev.* **112**, 3777–3807 (2012).
2. Canepa, P. *et al. J. Phys. Chem. C* **123**, 16843–16850 (2019).
3. Gys, N. *et al. Appl. Surf. Sci.* **566**, 150625 (2021).



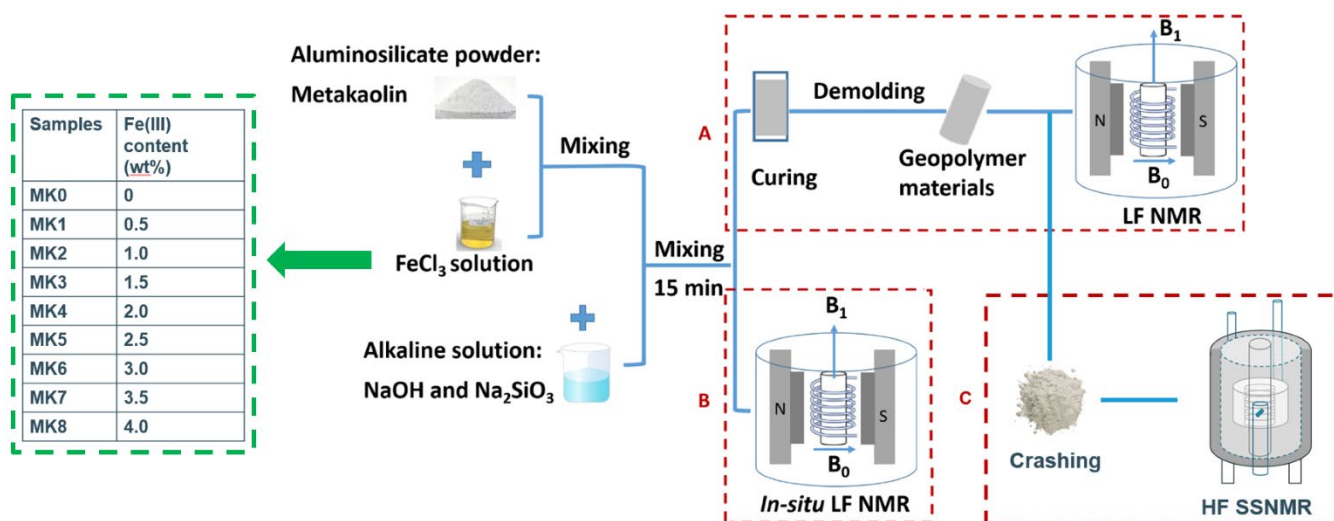
## Low field and high field NMR response on Fe<sup>3+</sup> loaded inorganic polymers

Z. Yu<sup>a,b</sup>, R. O. Silva<sup>a</sup>, Y. Pontikes<sup>b</sup>, D. Sakellariou<sup>a</sup>

<sup>a</sup>KU Leuven, M2S, CMAcs, Celestijnenlaan 200F, 3001 Heverlee, Belgium

<sup>b</sup>KU Leuven, Department of Materials Engineering, Kasteelpark Arenberg 44, 3001, Leuven, Belgium

Low field nuclear magnetic resonance (LF NMR) relaxometry and high field (HF) solid-state NMR spectrometry have proven to be robust and versatile tools for probing pore structures and molecular structures, respectively, in inorganic polymers (IPs). As sustainable construction materials, IPs take advantage of industrial waste as raw materials, which likely contain paramagnetic impurities, such as Fe<sub>2</sub>O<sub>3</sub>. The nuclear-electron interactions have great effects on spin relaxation and spectra features, e.g., linewidth and chemical shifts. These effects can lead to misinterpretation of NMR results. This work, for the first time, combines LF and HF solid-state NMR to investigate IPs loaded with various concentrations of ferric iron, and to reveal the influence of paramagnetic Fe<sup>3+</sup> on proton relaxation and spectra. Soluble FeCl<sub>3</sub> was introduced to provide active Fe<sup>3+</sup>, which can potentially incorporate into other species, such as SiO<sub>4</sub><sup>2-</sup>. The experimental procedure is depicted in Scheme 1. The LF NMR results demonstrate that (1) the longitudinal and transverse relaxation times ( $T_1$  and  $T_2$ ) linearly depend on pore diameter and are inversely proportional to the Fe<sup>3+</sup> content, (2) the soluble Fe<sup>3+</sup> has an insignificant effect on spin relaxation over the entire studied range of Fe<sup>3+</sup> content because the surface relaxivities ( $\rho_1$  and  $\rho_2$ ) only vary by a factor of  $\sim 1.5$ , and (3)  $T_2$  dynamics has proven to be an effective method to describe the geopolymerization kinetics, while  $T_2$  at different stages is affected by Fe<sup>3+</sup> to various degrees. The results of HF solid-state NMR confirm that the introduction of Fe<sup>3+</sup> resulted in intensity weakening and linewidth broadening in the observed spectra. In addition to the asymmetric broadening due to structural alteration, symmetric broadening in the less polymerized Q species (e.g. Si(0Al), Si(1Al), and Si(2Al)) was also observed. The latter is an indication that the influence of paramagnetic ions affects more the less polymerized Q species rather than the high cross-linked Q species, such as Si(3Al) and Si(4Al).



Scheme 1 The schematic plot of the experimental procedure. Metakaolin-based IPs loaded with various amounts of Fe<sup>3+</sup> were synthesized by mixing metakaolin with FeCl<sub>3</sub> solutions and alkaline activators. (A) The mixtures were cast into a silicone mold and cured for 20 h at 40 °C, followed by the LF NMR measurements (1D  $T_1$   $T_1$  and  $T_2$   $T_2$  relaxation times and 2D  $T_1$   $T_1$  -  $T_2$  $T_2$  correlations) after demolding. (B) The mixtures were loaded into an NMR Teflon mold and immediately transferred into the closed NMR chamber to *in-situ* record the  $T_2$   $T_2$  relaxation time during the curing period (28 °C). (C) The cured samples were crashed before being packed into the rotor for HF solid-state NMR measurements.

## Characterization of tumor heterogeneity using multi-parametric MRI and unsupervised classification methods

M. Pusovnik<sup>\*1</sup>, S. Belderbos<sup>\*1</sup>, J. Wouters<sup>1</sup>, S. Van Huffel<sup>2</sup>, A. Croitor Sava<sup>1</sup>, W. Gsell<sup>1</sup> and U. Himmelreich<sup>1</sup>

<sup>1</sup> Department of Imaging & Pathology, Biomedical MRI, KU Leuven;

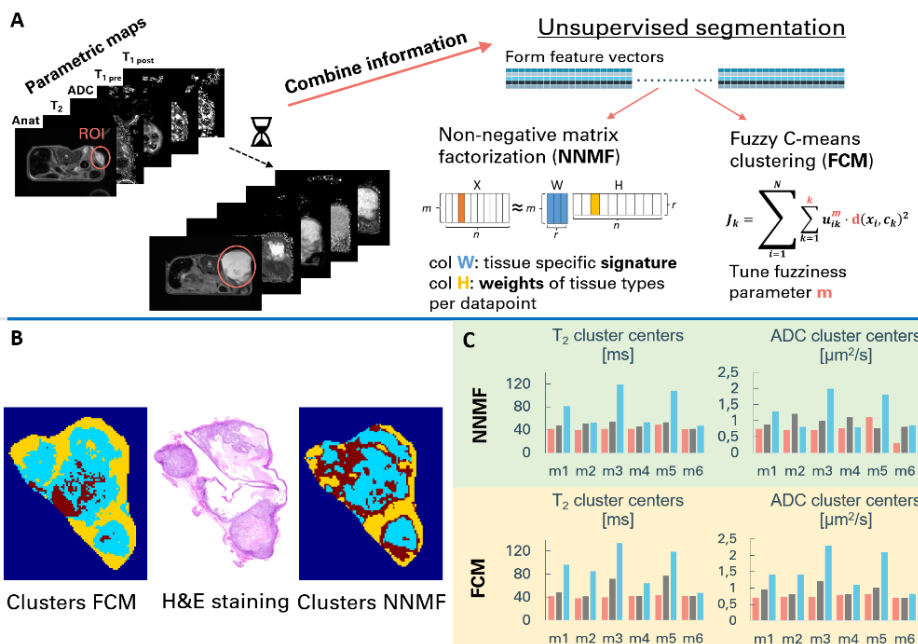
<sup>2</sup> Department of Electrical Engineering (ESAT), KU Leuven;

\* Authors contributed equally

An improved understanding of the dynamic tumor microenvironment, including vascularization and metabolism, can provide valuable information on the potential need to adapt experimental planning or on the biological effects of anti-cancer treatments. *In vivo* knowledge of the spatial distribution of viable, necrotic, and hypoxic areas within the tumor tissue can provide prognostic value in longitudinal studies. We aim to extract different tissue biomarkers by utilizing an *in vivo* multiparametric MRI (mpMRI) approach. Different techniques (T1, T2, contrast, diffusion, perfusion) yield complementary quantitative parameters that reflect specific aspects of the underlying tumor tissue biology. Combining this information aids in tissue characterization to confirm presence of different tissue types and allows close monitoring of the tumor growth from a molecular perspective. As a tumor model human ovarian SKOV-3 xenografts were generated in Swiss nude mice. Mice (n=6) were scanned weekly (w=6) using a Bruker Biospin 9.4T MRI. The general workflow is shown in Fig.1A. Parametric maps were generated with a standard non-linear least squares fit approach using Matlab. Multimodal image registration, as the intrinsically difficult step in such studies, was achieved with Elastix and Melastix using the mutual information metric with an affine transformation model. Tumor ROIs were manually delineated. Stacks of all parametric maps were jointly used in tissue characterization. Unsupervised classification method Fuzzy C-means (FCM), together with Non-Negative Matrix Factorization (NNMF) as a blind source separation technique, were tested in segmenting the tissue in different types. NNMF was chosen as shown to be superior in segmenting brain tumors in our previous similar study<sup>1</sup>. Results obtained report high spatial and temporal heterogeneity in the majority of animals. Clusters obtained with FCM and NNMF outline different spatial distributions (Fig. 1B), although with similar cluster centroid values (Fig. 1C). This suggests that this tumor model represents a very interwoven tissue mixture with only one distinct multimodal tissue footprint. Correlation with a detailed histopathological analysis for further ground-truthing is in progress. In conclusion, the developed image processing framework allows longitudinal follow-up of tumor development. In contrast to many experimental studies that only evaluate tumor size, using

paired mpMRI information may be of added value when selecting the time point to test new drugs in longitudinal preclinical studies.

1. Sauwen, N et al. "Comparison of unsupervised classification methods for brain tumor segmentation using multi-parametric MRI." *NeuroImage. Clinical* vol. 12 753-764. 2016



**Rapid structural elucidation of cyclic lipopeptides via NMR fingerprint matching**

V. De Roo<sup>1</sup>, Y. Verleysen<sup>1,4</sup>, B. Kovács<sup>1</sup>, R. De Mot<sup>2</sup>, M. Höfte<sup>3</sup>, A. Madder<sup>4</sup>, N. Geudens<sup>1</sup>, J.C. Martins<sup>1</sup>

<sup>1</sup> *NMR & Structure Analysis Unit, Department of Organic and Macromolecular Chemistry, Ghent University*

<sup>2</sup> *Centre of Microbial and Plant Genetics, Faculty of Bio-engineering, KU Leuven*

<sup>3</sup> *Laboratory of Phytopathology, Faculty of Bioscience Engineering, Ghent University*

<sup>4</sup> *Organic and Biomimetic Chemistry Research Group, Department of Organic and Macromolecular Chemistry, Ghent University*

Cyclic lipopeptides (CLiPs) are secondary metabolites that are produced and secreted by a range of bacterial genera including *Pseudomonas* and *Bacillus*. They are composed of an oligopeptide, cyclized through a lactone (depsi) bond, and capped at the N-terminus by a fatty acid moiety. Well over 100 CLiPs originating from *Pseudomonas* spp. have been described at varying levels of structural and biological activity details and their numbers keep rising. Structural variations are very diverse, including total amino acid sequence length, size of the macrocycle, amino acid identity and stereochemistry (e.g. D- vs. L-amino acids). In general, CLiPs are involved in several secondary functions and have been reported to display a range of antagonistic properties. Recently, the antimicrobial activities of *Pseudomonas* CLiPs were thoroughly reviewed. [1]

CLiPs and their producing bacteria are ubiquitous in Nature and reports detailing the discovery of novel or already characterized CLiPs from new sources appear regularly in literature. However, the lack of characterisation detail threatens to cause considerable confusion. Using NMR fingerprint matching, we have introduced a rapid and easy way of characterizing existing CLiPs coming from novel bacterial sources. Using this approach, the identity of CLiPs can be established by simple comparison of their NMR spectral fingerprint recorded under standardized conditions. Future integration of the spectral fingerprints into a publically accessible database should allow structure elucidation to be readily achieved by the wider scientific community involved in CLiP research.

1. Geudens, N.; Martins, J.C. *Front. Microbiol.* 2018, 9, 10.3389/fmicb.2018.01867.



## Additive manufacturing for the fabrication of subject-specific MRI passive shim and RF coil configurations

H. Vanduffel<sup>1</sup>, C. Parra<sup>1</sup>, W. Gsell<sup>2</sup>, R. de Oliveira Silva<sup>1</sup>, U. Himmelreich<sup>2</sup>, W. Vanduffel<sup>3</sup>, D. Sakellariou<sup>1</sup>, R. Ameloot<sup>1</sup>

<sup>1</sup> Microbiële en Moleculaire Systemen, <sup>2</sup> Beeldvorming & Pathologie, <sup>3</sup> Neurowetenschappen KULeuven, Leuven

The absence of subject-specific hardware components such as RF coils and passive shim configurations can be an important factor contributing to limited signal-to-noise ratios (SNR) in magnetic resonance applications. Additive manufacturing or 3D printing techniques are cost- and time-efficient, fully automated, digital manufacturing methods particularly suitable for the fabrication of subject-specific parts.

Patient-induced B<sub>0</sub> inhomogeneities are an important factor significantly affecting the imaging quality in terms of signal-to-noise ratio (SNR) and geometric distortion.[1][2] Since anatomical features are highly subject-specific, so are the type and extent of the magnetic field distortions. Traditional passive shims are constructed by placing ferro-, dia- or paramagnetic materials at discrete locations inside the magnet bore in an iterative process.[1][3] This time-consuming process has difficulties rendering the higher-order spherical harmonics (SHs) terms required to shim field inhomogeneities induced by complex anatomical features. We developed a powder-binder jetting technique to manufacture subject-specific passive shims (XYZ resolution = 300 μm; **fig 1A-B**). The method deposits variable concentrations of magnetic ink at precise pre-calculated positions (linear programming optimization algorithm) in a patient-specific shim design to sculpt B<sub>0</sub> towards a target distribution via the passive response of the 3DP shims to B<sub>0</sub>. Shim designs producing discrete SH terms (0th, 1st, and 2nd order) were fabricated as a proof-of-concept, and their response to a B<sub>0</sub> field of 9.4 T was analyzed using B<sub>0</sub> maps (**fig 1C**).

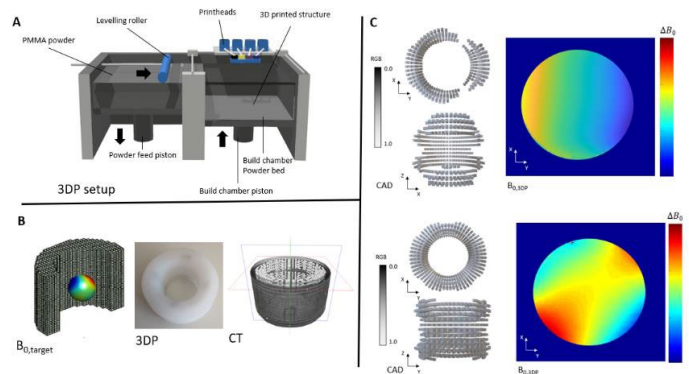


Figure 1: (A) Powder-binder jetting 3D printer (B) (Left to right:) Target B distribution with surrounding shim voxels; 3DP passive shim; CT reconstruction of 3D printed ferromagnetic distribution inside 3DP shim (C) Ferromagnetic distribution and B<sub>0</sub> map of 1st order SH (top) and 2nd order SH (bottom)

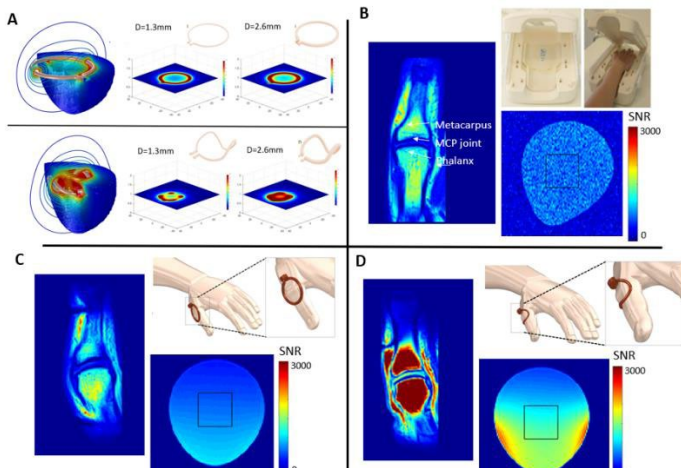


Figure 2: (A) EM simulations of non-conform (top) and subject-conform (bottom) RF coil; SNR map of MCP joint and phantom with: (B) commercial 16 channel coil; (C) non-conform Cu single loop RF coil; (D) subject-conform liquid-metal-injection single loop 3D-printed RF coil

A poor geometrical fit between the RF coil and subject also limits SNR.[4] Several approaches relying on flexible coil substrates have shown promising results.[5]–[8] However, the flexibility hinders the precise and reproducible coil placement on the subject. We developed a 3D-printing-based manufacturing method for the fabrication of patient-specific RF coils. The seamless transition between digital and physical objects allows for integrating electromagnetic simulations prior to fabrication (**fig 2A**), facilitating design iterations. Proof-of-concept 3D-printed subject-conform coils were fabricated to image a human thumb's metacarpophalangeal (MCP) joint. SNR gains of 35% for the 3D subject-specific liquid-metal-injected coil (**fig 2D**) were obtained compared to the state-of-the-art commercial 16 channel hand/wrist array (**fig 2B**) as a result of the improved filling factor. The non-conform copper wire coil showed a decrease in SNR of 16% (**fig 2C**)

The results discussed above demonstrate how 3D printing can be exploited as a time- and cost-efficient manufacturing method to fabricate subject-specific MRI hardware components, significantly increasing image quality in terms of SNR and geometric distortions.

[1]K. Wachowicz, "Evaluation of active and passive shimming in magnetic resonance imaging," Res. Reports Nucl. Med., no. October, p. 1, 2014.[2]J. P. Stockmann and L. L. Wald, "NeuroImage In vivo B<sub>0</sub> field shimming methods for MRI at 7 T," Neuroimage, vol. 168, no. June 2017, pp. 71–87, 2018.[3]S. Yang, H. Kim, M. Ghim, B. Lee, and D. Kim, "Local in vivo shimming using adaptive passive shim positioning ☆," Magn. Reson. Imaging, vol. 29, no. 3, pp. 401–407, 2011. [4]B. Gruber, M. Froeling, T. Leiner, and D. W. J. Klomp, "RF coils: A practical guide for nonphysicists," J. Magn. Reson. Imaging, vol. 48, no. 3, pp. 590–604, 2018.[5]J. A. Nordmeyer-Massner, N. De Zanche, and K. P. Pruessmann, "Stretchable coil arrays: Application to knee imaging under varying flexion angles," Magn. Reson. Med., vol. 67, no. 3, pp. 872–879, 2012. [6]J. A. Malko, E. C. McClees, I. F. Braun, P. C. Davis, and J. C. Hoffman, "A flexible mercury-filled surface coil for MR imaging," Am. J. Neuroradiol., vol. 7, no. 2, pp. 246–247, 1986. [7]G. Adriany et al., "A geometrically adjustable 16-channel transmit/receive transmission line array for improved RF efficiency and parallel imaging performance at 7 Tesla," Magn. Reson. Med., vol. 59, no. 3, pp. 590–597, 2008. [8]J. R. Coreia et al., "Screen-printed flexible MRI receive coils," Nat. Commun., vol. 7, pp. 1–7, 2016.

## A unique quantitative $^1\text{H-NMR}$ approach for lung cancer detection using a plasma protein-binding competitor

E. Derveaux<sup>1</sup>, M. Thomeer<sup>1,2</sup>, L. Mesotten<sup>1,3</sup>, G. Reekmans<sup>4</sup> and P. Adriaensens<sup>4</sup>

*1 Faculty of Medicine and Life Sciences, Hasselt University, Hasselt*

*2 Department of Respiratory Medicine, Ziekenhuis Oost-Limburg, Genk*

*3 Department of Nuclear Medicine, Ziekenhuis Oost-Limburg, Genk*

*4 Applied and Analytical Chemistry, Institute for Materials Research, Hasselt University, Diepenbeek*

Metabolite profiling of human blood plasma by proton nuclear magnetic resonance ( $^1\text{H-NMR}$ ) spectroscopy offers great potential for early cancer diagnosis and unraveling disruptions in cancer metabolism. Despite the essential attempts to standardize pre-analytical and external conditions, such as buffer pH or measurement temperature, the donor-intrinsic plasma protein concentration of human serum albumin (HSA) is highly overlooked. However, this is of utmost importance, since several plasma metabolites bind to HSA, resulting in an underestimation of the metabolites' signal intensities and chemical shift fluctuations. Our research group developed a novel  $^1\text{H-NMR}$  approach to avoid HSA-metabolite binding by adding 4 mM trimethylsilyl-2,2,3,3-tetradeuteriopropionic acid (TSP) as a strong binding competitor<sup>1</sup>. In addition, it is demonstrated, for the first time, that maleic acid is a reliable internal standard to quantify the human plasma metabolites without the need for protein precipitation. Metabolite spiking is further used to identify the peaks of 62 plasma metabolites and to divide the  $^1\text{H-NMR}$  spectrum into 237 well-defined integration regions, representing these 62 metabolites. The large majority of these regions are showing a small intrasample variability with only a %RSD <5%, thus indicating the high robustness level of the protocol.

The methodology is validated for clinical applicability as well, by showing a metabolism-based differentiation between lung cancer patients and healthy controls in a large patient cohort ( $n = 160$ ). Hereto, a supervised multivariate classification model is trained using the intensities of these integration regions (areas under the peaks) that are normalized against the maleic acid signal. The model allows discrimination between the two groups with a specificity, sensitivity, and area under the curve of 93%, 85%, and 0.95, respectively. Finally, the robustness of the trained classification model is shown by additional external validation in an independent patient cohort ( $n = 72$ ).

1. Derveaux, E., Thomeer, M., Mesotten, L., Reekmans, G. and Adriaensens, P. *Metabolites* 2021, **11**, 537.

## Pitfalls in sample preparation of metalloproteins for low-temperature EPR: the example of alkaline myoglobin

I. Serra<sup>1,2</sup>, I. García Rubio<sup>2,3</sup> and S. Van Doorslaer<sup>1</sup>

<sup>1</sup> Department of Chemistry, University of Antwerp, Antwerp, Belgium.

<sup>2</sup> Department of Condensed Matter Physics, University of Zaragoza, Zaragoza, Spain.

<sup>3</sup> Centro Universitario de la Defensa, Zaragoza, Spain.

Due to fast relaxation processes of transition metal ions, electron paramagnetic resonance (EPR) spectroscopy of metalloproteins needs to be performed at cryogenic temperatures. To avoid damaging the biological system upon freezing, a cryoprotectant is generally added to the sample as a glassing agent [1]. Even though cryoprotectants are expected to be inert substances, evidences in literature show their non-innocent role in altering the shape of EPR spectra of proteins and biological objects in general. In this work we conduct a systematic study on the impact of several experimental factors—such as buffer composition, choice of cryoprotectant, pH and temperature—on the EPR spectrum of myoglobin, taken as a reference system for being a well-characterized heme-containing protein. We focus on high-pH buffers to induce and investigate the alkaline transition of ferric myoglobin (pKa ~ 8.9). A combined approach of continuous-wave EPR and UV–visible absorption spectroscopy shows that using particular pairs of buffers and cryoprotectants determines a considerable pH variation in the sample and that this effect is enhanced at cryogenic temperature. In addition, phase memory times were measured to evaluate the efficiency of different cryoprotectants and compared with spectral linewidths in continuous-wave EPR. Our findings suggest that among the selected cryoprotectants ethylene glycol is rather effective, even more than the widely used glycerol, without having unwanted effects [2].

1. Russell D.S., *Physical Methods for Chemists*, 2nd edn. (Surfside Scientific Publishers, Gainesville, 1992)

2. Serra, I., García Rubio, I. & Van Doorslaer S., *Appl. Magn. Reson.* 2021.

## NMR as a versatile tool to investigate supramolecular hydrogelation

R. Van Lommel<sup>1,2</sup>, J. Van Hooste<sup>1</sup>, J. Vandaele<sup>3</sup>, G. Steurs<sup>1</sup>, T. Van der Donck<sup>4</sup>, F. De Proft<sup>2</sup>, M. Alonso<sup>2</sup>, S. Rocha<sup>3</sup>, D. Sakellariou<sup>5</sup> and W. M. De Borggraeve<sup>1</sup>

<sup>1</sup> *Molecular Design and Synthesis, Department of Chemistry, KU Leuven.*

<sup>2</sup> *Eenheid Algemene Chemie, Department of Chemistry, Vrije Universiteit Brussel.*

<sup>3</sup> *Molecular Imaging and Photonics, Department of Chemistry, KU Leuven.*

<sup>4</sup> *Department of Materials Engineering, KU Leuven.*

<sup>5</sup> *Centre for Membrane Separations, Adsorption, Catalysis and Spectroscopy for Sustainable Solutions, Department of Microbial and Molecular Systems, KU Leuven.*

From the beginning of the 21<sup>st</sup> century onwards, supramolecular hydrogels have garnered significant attention as a next-generation soft material.<sup>1</sup> Potential applications of these materials range from drug delivery systems to oil-spillage remediating agents and are enabled by their noncovalent driven self-assembly. An adequate understanding of the gelation mechanism benefits the development of new supramolecular gels, and for this reason several experimental techniques have been applied to probe the gelation mechanism. Among these techniques, NMR experiments have been used to investigate changes in chemical shifts or NMR relaxation times that occur during supramolecular gelation, from which insights can be obtained regarding the self-assembly process.<sup>2,3</sup> However, due to the viscoelastic nature of these supramolecular gels, it is challenging to find out which material phase the gelator molecules that generate the NMR signals find themselves in.

In this talk, we will present how variable temperature NMR experiments allowed us to explain the gelation mechanism of a bis-urea-based small molecule in water. Crucially, ERETIC2 experiments enabled the quantification of the sol-to-gel transition, without perturbing the system. By complementing these results with single-particle tracking experiments and scanning electron microscopy imaging, a stepwise self-assembly mechanism is proposed in which spherical particles mature into a nanofibrous network (Figure 1).

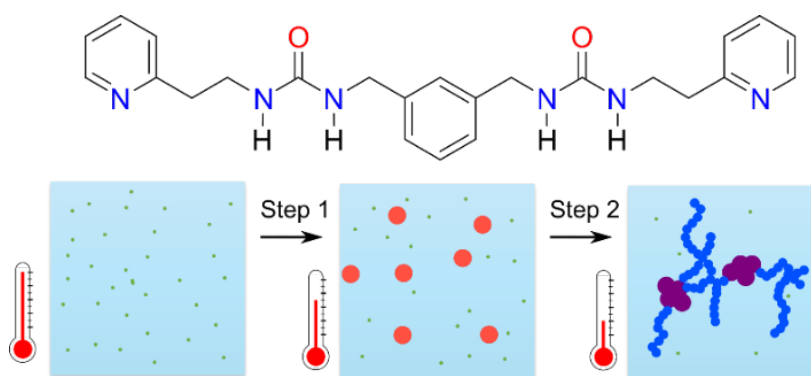


**Figure 1.** Schematic representation of a stepwise supramolecular sol-to-gel transition of a bis-urea-based molecule in water.

1. Sangeetha, N. M. and Maitra, U. *Chem. Soc. Rev.* 2005, **34**, 821-836.
2. Escuder, B., Llusar, M. and Miravet, J. F. *J. Org. Chem.* 2006, **71**, 7747-7752.
3. Hirst, A. R., Coates, I. A., Boucheteau, T. R., Miravet, J. F., Escuder, B., Castelletto, V., Hamley, I. W. and Smith, D. K. *J. Am. Chem. Soc.* 2008, **130**, 9113-9121.

## Posters



## Low resolution nuclear magnetic resonance for the study of nickel (II) and manganese (II) removal by ion exchange resin.

M. Bernardi<sup>1</sup>, Y. Gossuin<sup>1</sup> and A.L. Hantson<sup>2</sup>.

<sup>1</sup>Biomedical Physics Department, Umons

<sup>2</sup>Chemical and Biochemical Engineering Department, Umons

Heavy metals discharged by industrial wastewater to the environment has become a major public health and environmental concern [1]. In this context, adsorption of metal present in wastewater by ion exchange resins or adsorbents is one of the most used methods. However, current techniques to study the adsorption efficiency are indirect and destructive.

In this research, the paramagnetic properties of Ni (II), Mn (II) present in wastewater are used. Indeed, it is well known that paramagnetic ions affect the Nuclear Magnetic Resonance (NMR) relaxation times of water protons, which can be measured by benchtop NMR relaxometry [2-3]. Therefore, the purpose of this study is to prove the abilities of direct and non-destructive NMR relaxometry to monitor the removal of paramagnetic heavy metals.

In order to study the adsorption kinetics, a sample containing a small amount of resin (Amberlite IR120) was put in contact with aqueous solutions containing the paramagnetic ion of interest before being shaken by a vortex mixer. The transverse relaxation time (T<sub>2</sub>) was measured at different time intervals which allowed the monitoring of the amount of adsorbed metal. Repeating the same experiment with different metal concentrations provided the adsorption isotherms.

The equilibrium adsorption behavior of all metal ions can be satisfactorily described by the Langmuir model, with maximum adsorption capacity of 84.1 mg g<sup>-1</sup> and 50.3 mg g<sup>-1</sup> for Ni (II) and Mn (II) respectively whereas the sorption equilibrium constant are 1.55 L mg<sup>-1</sup> (Ni (II)) and 40.2 L mg<sup>-1</sup> (Mn (II)). Experimental kinetic data fitted well with the pseudo-second-order kinetic model.

The next step will be to reproduce these experiments for other adsorbents and paramagnetic ions at different magnetic fields. With this methodology, the adsorption could be followed with low-cost portable NMR device. In the future, it will also be interesting to carry out a so-called NMR column experiment in order to investigate the adsorption within the resin in real-time.

[1] Tchounwou, P. B., Yedjou, C. G., Patlolla, A. K., & Sutton, D. J., *Molecular, Clinical and Environmental Toxicology. Experientia Supplementum*, 101, 133-164 (2012).

[2] Gossuin, Y., Hantson, A.-L., & Vuong, Q. L., *Journal of Water Process Engineering*, 33, 101024 (2020).

[3] Gossuin, Y., & Vuong, Q. L., *Separation and Purification Technology*, 202, 138-143 (2018).

This work was supported by the Fonds de la recherche scientifique-FNRS under Grant n° T.0113.20

## Impact of inhibition of the mitochondrial pyruvate carrier on the tumor extracellular pH as measured by CEST-MRI

C. Buyse<sup>1#</sup>, N. Joudiou<sup>2#</sup>, C. Corbet<sup>3</sup>, O. Feron<sup>3</sup>, L. Mignon<sup>1</sup>, J. Flament<sup>4</sup> and B. Gallez<sup>1,\*</sup>

<sup>1</sup> Louvain Drug Research Institute, Biomedical Magnetic Resonance, Université catholique de Louvain (UCLouvain), Brussels, Belgium

<sup>2</sup> Louvain Drug Research Institute, Nuclear and Electron Spin Technologies (NEST), platform, Université catholique de Louvain, Brussels, Belgium

<sup>3</sup> Pole of Pharmacology and Therapeutics (FATH), Institut de Recherche Expérimentale et Clinique (IREC), Université catholique de Louvain (UCLouvain), Brussels, Belgium

<sup>4</sup> Université Paris-Saclay, Commissariat à l'Energie Atomique et aux Energies Alternatives (CEA), Centre National de la Recherche Scientifique (CNRS), Molecular Imaging Research Center (MIRCen), Laboratoire des Maladies Neurodégénératives, Fontenay-aux-Roses, France

The acidosis of the tumor micro-environment may have profound impact on cancer progression and on the efficacy of treatments. In the present study, we evaluated the impact of a treatment with UK-5099, a mitochondrial pyruvate carrier (MPC) inhibitor on tumor extracellular pH (pHe).

Glucose consumption, lactate secretion and Extracellular acidification rate (ECAR) were measured in vitro after exposure of cervix cancer SiHa cells and breast cancer 4T1 cells to UK-5099 (10  $\mu$ M). Mice bearing the 4T1 tumor model were treated daily during four days with UK-5099 (3 mg/kg). The pHe was evaluated in vivo using either chemical exchange saturation transfer (CEST)-MRI with iopamidol as pHe reporter probe or <sup>31</sup>P-NMR spectroscopy with 3-aminopropylphosphonate (3-APP). MR protocols were applied before and after 4 days of treatment.

Glucose consumption, lactate release and ECAR were increased in both cell lines after UK-5099 exposure. CEST-MRI showed a significant decrease in tumor pHe of 0.22 units in UK-5099-treated mice while there was no change over time for mice treated with the vehicle. Parametric images showed a large heterogeneity in response with 16 % of voxels shifting to pHe values under 7.0. In contrast, <sup>31</sup>P-NMR spectroscopy was unable to detect any significant variation in pHe.

MPC inhibition led to a moderate acidification of the extracellular medium in vivo. CEST-MRI provided high resolution parametric images (0.44  $\mu$ l/voxel) of pHe highlighting the heterogeneity of response within the tumor when exposed to UK-5099.



## The use of cerebral perfusion MRI in a rat model to investigate the key role of microvascular rarefaction in the development of Vascular Cognitive Impairment

B. Callewaert<sup>1,2</sup>, W. Gsell<sup>1</sup>, E. A. V. Jones<sup>2,3,\*</sup> and U. Himmelreich<sup>1,\*</sup>

<sup>1</sup> Biomedical MRI Group, University of Leuven.

<sup>2</sup> Center for Molecular and Vascular Biology (CMVB), University of Leuven.

<sup>3</sup> School for cardiovascular diseases (CARIM), Maastricht University, The Netherlands.

The prediction, prevention, and detection of vascular cognitive impairment (VCI) remains challenging. Recently, reduced microvascular density, called microvascular rarefaction, and microvascular dysfunction were linked to the early development of VCI. Microcirculatory impairments result in altered microvascular perfusion and tissue oxygenation, which can ultimately lead to damage to the brain tissue. Microvessels however, are below the currently achievable spatial resolution of MRI and other clinically applicable imaging methods, making it impossible to perform direct measurement of the microvascular density. Nevertheless, cerebral perfusion MRI provides valuable insights into the cerebral microvascular function, integrity, and architecture in a non-invasive matter.

Using several perfusion MRI techniques, we aim to extract quantitative perfusion parameters, providing indirect measurement of the microvascular density in the rat brain. Pre-clinical protocols and post-processing pipelines for pseudo-continuous Arterial Spin Labelling (ASL), Automated Dynamic susceptibility contrast (DSC) and Intravoxel Incoherent Motion (IVIM) in rat brain were established, using a 9.4 T Bruker Biospin MR Scanner.

The proposed perfusion MRI protocol provides complementary read-outs and allows the cross-validation of the different cerebral perfusion methods. The obtained parameters from the less established IVIM technique ( $f$ ,  $D^*$ ) can be correlated to the classical perfusion parameters, obtained from the more conventional ASL and exogenous DSC approaches (CBF, CBV and MTT). The application of the proposed protocol in a rat model of VCI allows us to indirectly study the cerebral microcirculation, even at the developmental stages, before the onset of clinical symptoms.

In order to cross-validate our MRI measurements, we developed histological analysis of whole rat brain histological slices that generates quantitative data in voxel wise manner. This allows direct comparison of the perfusion MRI measurements to the in vivo vascular density. The investigation of the relationship between the MRI measurements and the histological changes in the microvascular density, could lead to a more comprehensive understanding of the physiological relevance of the observed changes in cerebral perfusion.

Figure1: Overview of the proposed method; A. perfusion MRI methods; B. quantification of the microvascular density using histology

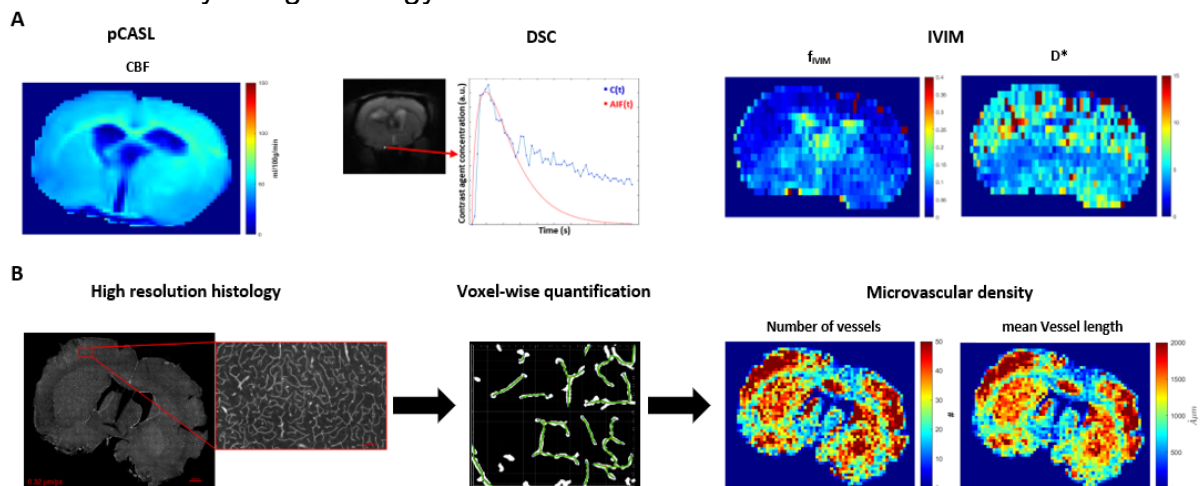


Figure1: Overview of the proposed method; A. perfusion MRI methods; B. quantification of the microvascular density using histology

**NMR studies of hydrogen-bonded water-aminium assemblies templating SAPO materials**

C. Vinod Chandran<sup>1,2</sup>, S. Radhakrishnan<sup>1,2</sup>, S. H. Park<sup>3</sup>, W. Choi<sup>3</sup>, K. C. Kemp<sup>3</sup>, R. G. Bell<sup>4</sup>, C. E. A. Kirschhock<sup>2</sup>, S. B. Hong<sup>3</sup>, E. Breynaert<sup>1,2</sup>

<sup>1</sup> NMRCoRe, Celestijnenlaan 200 F – box 2461, KU Leuven, 3001 Heverlee, Belgium

<sup>2</sup> Center for Surface Chemistry and Catalysis, Characterization and Application Team (COK-kat), Celestijnenlaan 200 F – box 2461, KU Leuven, 3001 Heverlee, Belgium

<sup>3</sup> Center for Ordered Nanoporous Materials Synthesis, Division of Environmental Science and Engineering, POSTECH, Pohang 37673, Korea

<sup>4</sup> Department of Chemistry, University College London, 20 Gordon Street, London WC1H 0AJ, UK

Water plays a central role in the crystallization of a variety of organic, inorganic, biological, and hybrid materials. This is also the case of hydrothermal synthesis of zeolites and zeolite-like materials, an important class of industrial catalysts and adsorbents. However, structure direction by water in zeolite synthesis has never been clearly elucidated. Here we report the crystallization of phosphorous-based molecular sieves using rationally designed, hydrogen-bonded water-aminium assemblies, resulting in molecular sieves with crystallographic ordering of heteroatoms. We demonstrate that an assembly of 1:1 water-diprotonated N,N-dimethyl-1,2-ethanediamine acts as a structure-directing agent in the synthesis of a silicoaluminophosphate material with phillipsite topology, with the help of X-ray crystallography and multinuclear solid-state NMR spectroscopy. This concept of structure direction by water-containing supramolecular assemblies should be applicable to the synthesis of many classes of porous materials.

## Relaxorption: a new in situ NMR measurement for adsorption

R. Oliveira-Silva<sup>1</sup>, J. Marreiros<sup>1</sup>, D. Sakellariou<sup>1</sup>, R. Ameloot<sup>1</sup>

<sup>1</sup>Centre for Membrane Separations, Adsorption, Catalysis and Spectroscopy for Sustainable Solutions (cMACS) – KU Leuven

Isotherm measurements, through adsorption of vapours/gases, is a standard technique for porous materials characterization. This technique relies on the quantification of adsorbed molecules in the porous matrix using bulk barometric, measured in the hole adsorption cell. The invaluable results obtained by this method provide different characteristics of the material, such as BET surface area and the maximum capacity of adsorption with limited information about the guest/host interaction energy. Lowfield NMR, on the other hand, can probe physicochemical characteristics of materials by the relaxation time distributions of molecules occupying their pores.[1,2]

In this work, we show the results obtained with an new integrated NMR/physorption setup, recording full in situ isotherms independently by both techniques. Applied to a set of Metal-Organic Frameworks, this double-barreled technique allowed identifying sorption sites, probing structural changes in the host, observing changes in the dynamics of the adsorbed molecules and calculating an interaction energy parameter.[2,3]

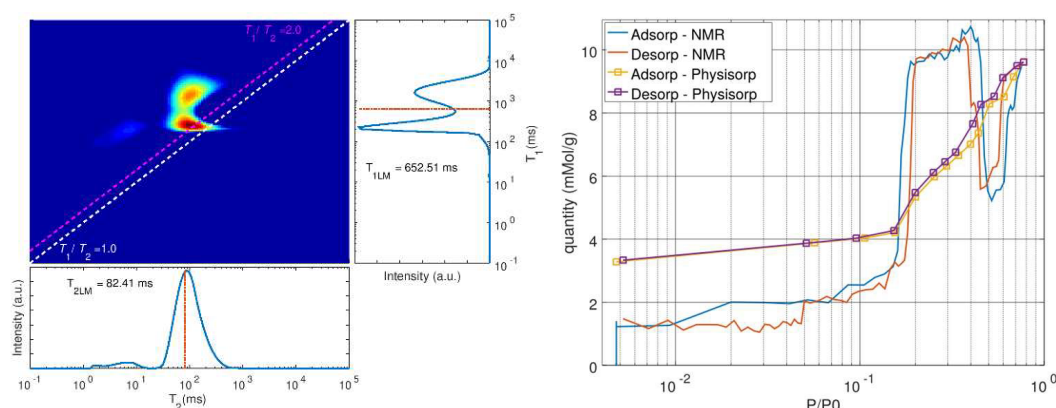


Figure 1 - Using the bi-dimensional  $T_1 \times T_2$  relaxation map in a) different sites for methanol adsorption were identified for the ZIF-8. The transitions between the narrow and large pore configurations are directly observed through the NMR signal in b) for the MIL-53(Al) during the ethanol isotherm.

- [1] Judeinstein, P. et al., *J. Magn. Reson.* 277, 25-29 (2017);  
 [2] D'Agostino, C. et al., *Chem. Eur. J.* 20, 13009-130015 (2014) ;  
 [3] Marreiros, J., Oliveira-Silva, R. et al., *JACS* 143, 8249-8254 (2021).

## Engineering microbial cells for the biosynthesis of novel anticancer agents

D. De Ruyscher<sup>1</sup>, E. Vriens<sup>1</sup>, G. Steurs<sup>2</sup>, W. De Borggraeve<sup>2</sup> and J. Masschelein<sup>1</sup>

<sup>1</sup> Laboratory for Biomolecular Discovery & Engineering, VIB-KU Leuven Center for Microbiology.

<sup>2</sup> Molecular Design and Synthesis, Chemistry Department, KU Leuven.

Natural products have historically been an important source of marketed drugs. Microorganisms can be efficient factories of bioactive molecules which possess impressive therapeutic potential in various diseases. *Pseudomonas* bacteria are known to produce such secondary metabolites which inspired researchers to analyse their genomes for finding interesting biosynthetic gene clusters (BGCs). These sets of genes encode for multienzyme complexes responsible for the construction of specialised compounds.

A novel hybrid modular polyketide synthase (PKS)-nonribosomal peptide synthetase (NRPS) assembly line was discovered wherein the individual enzymes perform several unique transformations.<sup>1</sup> The biosynthetic products of this assembly line belong to the benzolactone enamide class of natural products (Figure 1). They selectively inhibit the mammalian vacuolar (V-)ATPases which prevents tumour cell proliferation.<sup>2</sup> However, only three oximidines have originally been identified in literature whereas we observed additional analogues when analysing *Pseudomonas* extracts. They were separated using HPLC and LC/MS analysis revealed several recurring masses indicating the presence of several oximidine isomers. We are currently evaluating the feasibility of using DFT calculations of chemical shifts and coupling constants to help in the assignment of relative stereochemistries of these flexible molecules. The known Oximidine I (Figure 1) was identified via NMR as one of the oximidines present in the extract and serves as a case study. This work will be crucial in view of completely characterising other new oximidines as to date no crystal structures of these natural products have been reported and structure confirmation so far has happened via total synthesis.

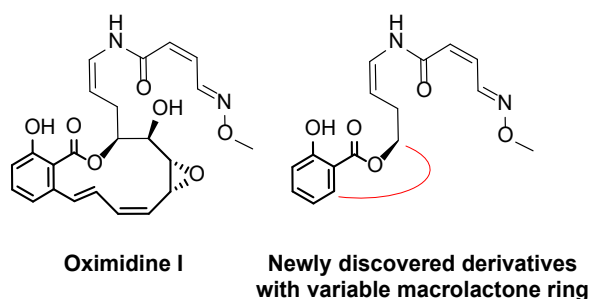


Figure 1: The molecular structure of the oximidines.

1. Fischbach, M. A. and Walsh, C. T. *Chem. Rev.* 2006, 106, 3468-3496.
2. Collins, M. P. and Forgac, M. *Biochim. Biophys. Acta Biomembr.* 2020, 1862, 183341.

**<sup>13</sup>C-MRS metabolic markers of response to targeted therapies in YUMM 1.7 melanoma xenografts**

C. Farah<sup>1</sup>, L. Mignon<sup>1,2</sup>, M.A. Neveu<sup>3</sup>, C. Bouzin<sup>4</sup>, F. Gourgue<sup>1</sup>, N. Joudiou<sup>1,2</sup>, C. Yelek<sup>1</sup>, J.-F. Baurain<sup>5</sup>, B. Jordan<sup>1,2</sup>

<sup>1</sup>Biomedical Magnetic Resonance (REMA) Group, Louvain Drug Research Institute, Belgium <sup>2</sup>Nuclear and Electron Spin Technologies (NEST) Platform, Louvain Drug Research Institute, Belgium

<sup>3</sup>Laboratory of Tumor Inflammation and Angiogenesis, Department of Oncology, KU Leuven, Belgium

<sup>4</sup>Université Catholique de Louvain, Institute de Recherche Expérimentale et Clinique, IREC Imaging Platform,

Belgium <sup>5</sup>Molecular Imaging and Radiation Oncology (MIRO) Group, Institute de Recherche Expérimentale et Clinique (IREC), Belgium

Melanoma is the most devastating form of skin cancer. <sup>1</sup>More than 50% harbour a BRAF V600E mutation. <sup>2</sup>The RAS/BRAF/MEK/ERK pathway is a central cancer driver with BRAF and MEK inhibitors combinations approved for clinical use. <sup>3</sup> Identification of biomarkers is needed to identify patients that are not responding to melanoma therapy, as well as for the development of potential metabolically targeted therapies. <sup>4</sup> <sup>13</sup>C-magnetic resonance spectroscopy (MRS) is a non-invasive tool able to assess tumor metabolism. In a recent study, we highlighted different metabolic shifts in melanoma cells in comparison with human melanoma xenografts. <sup>5</sup> <sup>6</sup> A potential factor that might be responsible for these *in vivo/in vitro* differences in metabolic behavior is the tumor microenvironment, including the immune system.

The aim of this work is to evaluate <sup>13</sup>C-MRS metabolic markers of response to targeted therapies in YUMM 1.7 syngeneic melanoma xenografts using *in vivo* hyperpolarized (HP) <sup>13</sup>C-pyruvate, and *ex vivo* U-<sup>13</sup>C-glucose 5-<sup>13</sup>C-glutamine, with the goal to improve melanoma treatment in the transition towards individualized therapy. For that purpose, we used *in vivo* hyperpolarized (HP) <sup>13</sup>C-pyruvate in C57B6J mice inoculated with YUMM1.7 melanoma cells. When tumors reached a volume of 300 mm<sup>3</sup>, they were treated with BRAFi (vemurafenib, 25mg/Kg) or with a combination of vemurafenib and trametinib (MEKi, 0.5mg/Kg) during 4 days. The glycolytic phenotype was assessed *in vivo* using HP <sup>13</sup>C-pyruvate, that was injected intravenously to tumor bearing mice to assess the <sup>13</sup>C-pyruvate/<sup>13</sup>C-lactate exchange.

We found that the tumor growth was significantly delayed in response to BRAF inhibition alone (relative growth delay factor (RGD)= 1.97, p=0.0421), to MEK inhibition alone (RGD= 3, p=0.0653), and more significantly in response to the combination of BRAF and MEK inhibition (RGD= 4.95, p=0.0022). Four out of five tumors showed a decrease in the lactate to pyruvate ratio in the combination group only, without reaching statistical significance. We observed a lack of change in MCT1 (monocarboxylate transporter-1) and MCT4 levels between Ctrl and BRAFi+MEKi group, in line with the lack of change in the <sup>13</sup>C-lactate to pyruvate ratio. Interestingly, we found a significant decrease in the <sup>13</sup>C lactate metabolites after U-<sup>13</sup>C-glucose infusion in treated group.

In conclusion, the decrease of <sup>13</sup>C lactate to <sup>13</sup>C pyruvate ratio did not reach a significant level and therefore disqualified HP <sup>13</sup>C pyruvate as a predictor of response to BRAF and MEK inhibition. <sup>13</sup>C-glucose feeding *in vivo* is more sensitive than HP <sup>13</sup>C-pyruvate to detect metabolic changes in response to BRAF/MEK inhibition in YUMM1.7 melanoma xenografts. The melanoma xenografts treated with BRAF/MEK inhibitors showed less lactate production and are therefore likely to be less glycolytic and respond to treatment. This should be confirmed after studying the expression of such glycolytic enzymes and transporters. The metabolic changes observed in response to treatments could be a potential therapeutic track to counteract the resistance to various therapies by targeting the metabolism. Further studies are needed to better understand the metabolic role in melanoma response to BRAF/MEK inhibitors.

1. Siegel, R. L., Miller, K. D. & Jemal, A. Cancer statistics, 2019. *CA. Cancer J. Clin.* **69**, 7–34 (2019).

2. Davies, H. *et al.* Mutations of the BRAF gene in human cancer. *Nature* **417**, 949–954 (2002).

3. Zhang, W. & Liu, H. T. MAPK signal pathways in the regulation of cell proliferation in mammalian cells. *Cell Res.* **12**, 9–18 (2002).

4. Brummer, C. *et al.* Metabolic targeting synergizes with MAPK inhibition and delays drug resistance in melanoma. *Cancer Lett.* **442**, 453–463 (2019).

5. Nelson, S. J. *et al.* DNP-Hyperpolarized <sup>13</sup>C Magnetic Resonance Metabolic Imaging for Cancer Applications. *Appl. Magn. Reson.* **34**, 533–544 (2008).

6. Kurhanewicz, J. *et al.* Hyperpolarized <sup>13</sup>C MRI: Path to Clinical Translation in Oncology. *Neoplasia N. Y.* **N 21**, 1–16 (2019).

7. Acciaro, S. *et al.* Metabolic imaging using hyperpolarized <sup>13</sup>C-pyruvate to assess sensitivity to the B-Raf inhibitor vemurafenib in melanoma cells and xenografts. *J. Cell. Mol. Med.* **24**, 1934–1944 (2020).

8. Acciaro, S. *et al.* Imaging markers of response to combined BRAF and MEK inhibition in BRAF mutated vemurafenib-sensitive and resistant melanomas. *Oncotarget* **9**, 16832–16846 (2018).

9. Meeth, K., Wang, J., Micevic, G., Damsky, W. & Bosenberg, M. W. The YUMM lines: a series of congenic mouse melanoma cell lines with defined genetic alterations. *Pigment Cell Melanoma Res.* **29**, 590–597 (2016).

## New Platforms Dedicated to MRI/PAI Bimodal Imaging: Molecular and Nanoparticular Approaches?

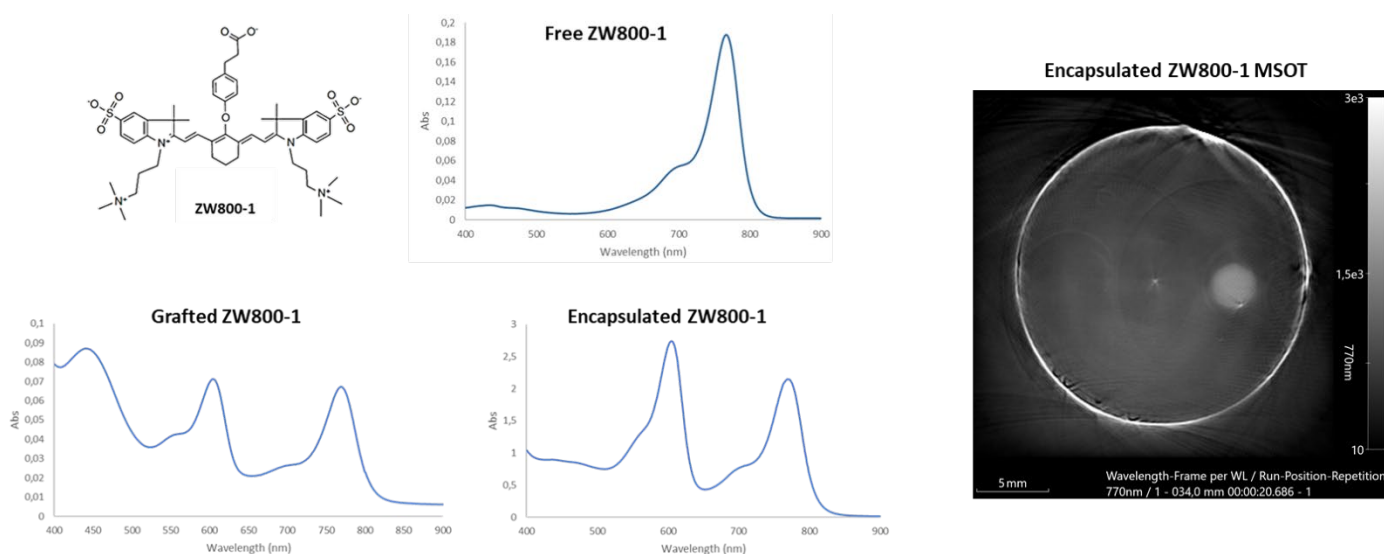
C. Gosée<sup>1,3</sup>, C. Cadiou<sup>3</sup>, J. Moreau<sup>3</sup>, M. Callewaert<sup>3</sup>, L. Larbanoix<sup>1,2</sup>, F. Chuburu<sup>3</sup>, S. Laurent<sup>1,2</sup>

1 General, Organic and Biomedical Chemistry Unit, NMR and Molecular Imaging Laboratory, University of Mons (UMONS), 7000 Mons, Belgium

2 Center for Microscopy and Molecular Imaging (CMMI), 6041 Gosselies, Belgium

3 Institut de Chimie Moléculaire de Reims, CNRS UMR 7312, University of Reims Champagne-Ardenne URCA, 51685 Reims Cedex 2, France.

The association of magnetic resonance imaging (MRI) with photoacoustic imaging (PAI) offers advantages in the medical field (faster detection of tumours, better understanding, and improvement of therapeutic protocols) owing to the excellent spatial resolution of the former technique and the high sensibility of the latter. This is the context of my thesis. For MRI imaging, T1 contrastophores (gadolinium chelates) will be used. For photoacoustic imaging, non-endogenous luminophores absorbing in the near infrared will be used. The NIR-absorbing luminophore used here is ZW800-1. The latter has been synthesised and fully characterised as shown in the presentation. The encapsulation of ZW800-1 within nanohydrogels, composed of chitosan and hyaluronic acid, was tested. To facilitate the formation of these nano-objects, ZW800-1 was grafted onto the CS backbone. Photophysical measurements were performed on free, grafted, and encapsulated ZW800-1 will be presented. For free ZW800-1, a single band was observed around 770 nm. For grafted and encapsulated ZW800-1, two bands were observed at 770 nm and 600 nm. To avoid this second band at 600 nm, purification tests are in progress. Preliminary optoacoustic experiments on nanoparticles have shown promising results as observed in the ghost images.





## Development of a combined methodology towards mechanistic investigation of rare metal-free, light activated catalysts

A. Guidetti<sup>1</sup>, K. Gadde<sup>2</sup>, H.Y.V. Ching<sup>1</sup>, G. Mitrikas<sup>3</sup>, B.U.W. Maes<sup>2</sup>, D.M. Murphy<sup>4</sup>, S. Van Doorslaer<sup>1</sup>

1) BIMEF Group, Department of Chemistry, University of Antwerp, Antwerpen, Belgium

2) ORSY Group, Department of Chemistry, University of Antwerp, Antwerpen, Belgium

3) Institute of Nanoscience and Nanotechnology, N.C.S.R. Demokritos, Athens, Greece

4) EPR/ENDOR Spectroscopy Group, Department of Chemistry, Cardiff University, Cardiff, Wales, United Kingdom

Photocatalysis has been an important research field in the last 40 years and has become increasingly more common as an easy way to obtain unusual reactivity and greener synthetic pathways. While compounds of rare transition metals such as ruthenium and iridium are commonly employed,[1] in recent years the interest has started to shift towards different photocatalysts, such as metal-free organic dyes and compounds containing more easily available transition metals, such as copper, which not only allow for more economically affordable catalysts but also open up reactions and selectivity that were previously inaccessible or unexplored.[2] In the frame of the European Programme MSCA-Horizon 2020 "Paramagnetic Species in Catalysis Research (PARACAT)" we are working to shed light on synthetic pathways that employ these alternatives. In this talk we will present the insight we were able to obtain for two different photocatalytic processes employing commercially available photosensitizers. These remarkable synthetic protocols can use visible light and green solvents, resulting in high yield and minimal waste products.[4] Our aim is to obtain important mechanistic insights through Stern-Volmer fluorescence quenching studies and EPR experiments, in order to optimize the reaction protocol and allow in the future for a rational approach to the development of similar syntheses. EPR spectroscopic and fluorescence results will be presented and related to different mechanistic proposals.

We gratefully acknowledge funding from Marie Skłodowska-Curie Joint Doctorate grant agreement No 813209.

[1] Prier, C.K.; Rankic, D. A.; MacMillan, D.W.C.; *Chem. Rev.* 2013, 113, 5322-5363.

[2] Romero, N.A.; Nicewicz, D.A.; *Chem. Rev.* 2016, 116, 10075-10166.

[3] Mampuys, P.; Zhu Y.; Sergejev, S.; Ruijter, E.; Orru, R.V.A.; Van Doorslaer, S.; Maes, B.U.W.; *Org. Lett.* 2016, 18, 2808-2811.

[4] Gadde, K.; Mampuys, P.; Guidetti, A.; Ching, H.Y.V.; Herrebout, W.A.; Van Doorslaer, S.; Tehrani, K.A.; Maes, B.U.W.; *ACS Catalysis* 2020, 10, 15, 8765–8779

## P10

**Petrophysical characterization and shale-gas potential of the Late Paleocene Patala Formation, Potwar Basin, Pakistan (Eastern Tethys): Comparative study on porosity distribution in mudstones**

N. Khan<sup>1,2</sup>, H. Claes<sup>1</sup>, R. de Oliveira-Silva<sup>3</sup>, G. J. Weltje<sup>1</sup>, D. Sakellariou<sup>3</sup> and R. Swennen<sup>1</sup>

<sup>1</sup>*Department of Earth and Environmental Sciences, KU Leuven, Celestijnenlaan 200E, Leuven 3001.*

<sup>2</sup>*Department of Geology, University of Malakand, Chakdara 18800, Khyber Pakhtunkhwa, Pakistan.*

<sup>3</sup>*Department of Microbial and Molecular Systems (M<sup>2</sup>S), KU Leuven, Celestijnenlaan 200F, Leuven 3001.*

Pore network characterization is fundamental in both conventional and unconventional reservoirs owing to the storage and flow capacities of hydrocarbons. However, such characterization remains enigmatic in unconventional shale-gas reservoirs due to their ultra-fine grained texture, a broader range of pore sizes, heterogeneous composition and ultra-tight nature of pores. Thus, an integrated approach including water immersion porosimetry (WIP), nuclear magnetic resonance (NMR) relaxometry and mercury injection capillary pressure (MICP), coupled with X-ray diffraction and organic matter analyses was applied to capture the porosity distribution and petrophysical characteristics of the Late Paleocene Patala Formation in the Potwar Basin of Pakistan. NMR results show variation in porosity distribution, largely constrained by clay composition, organic matter enrichment and occurrence of pyrites. The pore size distribution and pore throats radii are estimated using MICP curves to predict pore network and reservoir quality. The former distribution illustrated that micro-, meso- and macro-pores predominates the porous volume of the formation. The porous volume is mainly dominated by a bi-modal distribution of pores as deduced from NMR. The organic-rich shale intervals hold more promising porosity and permeability compared to organic-lean samples and provide more space for shale-gas accumulation and preservation. The WIP, NMR and MICP porosities possess 1:1 linear relationships except for smectite-rich samples that underestimate the NMR porosity largely due to clay bound water within the smectite pore network. This implies based on the results of this study that the organic-rich shale intervals holding optimal porosity and connected pore spaces may act as “sweet spots” for shale-gas exploration in the Potwar Basin of Pakistan and analogous settings elsewhere. This study agrees with the traditional applications of NMR in porosity estimation for optimized shale-gas extraction but with a caution related to clay composition that underestimates the porosity.



## Simulation of Nuclear Magnetic Relaxation Induced by Superparamagnetic Nanoparticles trapped in a biological tissue

E. Martin<sup>1</sup>, Y. Gossuin<sup>1</sup>, Q. L. Vuong<sup>1</sup>

<sup>1</sup> Biophysics unit, UMONS, Mons.

Superparamagnetic nanoparticles are generally small bids of iron oxides and notably have a high magnetization when submitted to a high external field, and no remnant magnetization in zero field. Those properties make them suitable to be used as contrast agents in nuclear magnetic resonance, where they can accumulate in a tissue, affect its relaxation time, and therefore make it appear clearly in contrast to other surrounding tissues.

There is a variety of theoretical models which try to quantitatively explain the relaxation induced by those types of nanoparticles: it appears to be caused by the diffusion of the water molecules in the magnetic inhomogeneities that the nanoparticles produce in the sample [1].

The diffusion coefficient of water molecules therefore is an important parameter in these models. However, they only focus on relaxation in a homogeneous medium, whereas in a biological tissue, the diffusion of the water molecules is strongly constrained by the presence of a network of cells in which water diffuses. In particular, cellular membranes affect the water molecule movement through their permeability. Those constraints on diffusion affect the relaxation times [2].

This work aims at simulating by using Monte Carlo techniques the relaxation of water molecules in a tissue loaded with superparamagnetic nanoparticles. The cell network is modeled as a periodic layout of semi-permeable membranes.

It is shown that, when all the cells are identically loaded by the nanoparticles, the simulated relaxation times do not differ from the relaxation in a homogeneous medium and do not depend on the cell permeability. However, if the cells are not all loaded in the same way, that is to say, the nanoparticle load in the tissue is inhomogeneous, the relaxation can greatly vary and will depend on the cell permeability, and the spatial distribution of the nanoparticles. This effect should thus be taken into account for the iron quantification by MRI in vivo.

[1] Q. L. Vuong, P. Gillis, A. Roch, et Y. Gossuin, « Magnetic resonance relaxation induced by superparamagnetic particles used as contrast agents in magnetic resonance imaging: a theoretical review », Wiley Interdiscip. Rev. Nanomed. Nanobiotechnol., vol. 9, n o 6, p. e1468, nov. 2017.

[2] A. Szafer, J. Zhong, et J. C. Gore, « Theoretical Model for Water Diffusion in Tissues », Magn. Reson. Med., vol. 33, n o 5, p. 697-712, mai 1995.

### Trace level detection and quantification of crystalline silica in an amorphous silica matrix with natural abundance $^{29}\text{Si}$ NMR

S. Radhakrishnan,<sup>1,2</sup> H. Colaux,<sup>2</sup> C. Vinod Chandran,<sup>1,2</sup> D. Dom,<sup>1,2</sup> L. Verheyden,<sup>2</sup> F. Taulelle,<sup>1,2</sup> J. A. Martens,<sup>1,2</sup> and E. Breynaert<sup>1,2</sup>

<sup>1</sup> NMRCoRe, KU Leuven

<sup>2</sup> Center for Surface Chemistry and Catalysis – Characterization and Application Team (COK-KAT), KU Leuven.

Amorphous silica is commonly used in large scale applications: as desiccant, as filler in elastomers, for controlled release of drugs or as component in pest control systems. Quartz and other crystalline forms of silicon dioxide ( $\text{SiO}_2$ ), on the contrary, are known to cause lung cancer. European Union regulations, require silica gel manufacturers to certify the absence of crystalline  $\text{SiO}_2$  in their products, defining a maximum allowed concentration of 0.1%wt. Measurement of such low concentrations by standard lab-scale X-ray diffraction techniques is difficult due to sensitivity issues and require higher photon flux sources like in a synchrotron. Here we report on a protocol for the detection by solid state NMR spectroscopy under magic angle spinning conditions, of trace amounts of quartz in amorphous silica gels. Using  $^{29}\text{Si}$  MAS NMR spectroscopy with Carr-Purcell-Meiboom-Gill (CPMG) acquisition scheme and standard addition of crystalline quartz, quantitative detection of quartz concentrations up to 0.1 %wt. was achieved. This acquisition scheme takes the advantage of the long  $T_2$ , to refocus the magnetization using a sequence of  $180^\circ$  pulses at specific intervals (Figure 1). It allows to record the signal multiple times in a single scan, for acquisition times longer than the usual free induction decay (FID) observed following the direct-excitation measurement, thus increasing the total signal acquired per scan and in turn yielding a higher signal to noise ratio (SNR) per unit time. Fourier transformation of the train of CPMG echoes, leads to splitting of NMR pattern into a series of sharp peaks separated by a constant value ( $1/\tau$ ), referred to as “spikelets” (Figure 1). This train of echoes can be used as it is, taking advantage of the narrow peak width, or can be summed and Fourier transformed to obtain the regular-looking NMR spectrum. In addition, CPMG enables  $T_2$  filtering, i.e., by choosing a long enough echo delay (time between subsequent  $180^\circ$  pulses), components exhibiting a short  $T_2$  can selectively be removed from the spectrum to obtain spectra containing only the component with the longest  $T_2$ , that is, the signal from the crystalline sample. CPMG permitted to suppress the amorphous silica derived signal, benefitting from the extremely long  $T_2$  relaxation time of quartz in  $^{29}\text{Si}$ , and hence dramatically increasing the sensitivity. Significant reduction of the error in the determination of the integrated intensity was achieved by a point-by-point multiplication of all processed spectra (after corrections for the phase and for the drift of the static magnetic field) by a comb of Gaussian functions centred on the chemical shift range of quartz. significantly reduce the error in the determination of the integrated intensity by a point-by-point multiplication of all processed spectra (after corrections for the phase and for the drift of the static magnetic field) by a comb of Gaussian functions centred on the chemical shift range of quartz. These acquisition and dedicated post-processing method allowed to probe the near-absence of quartz in commercial, 100 % silica samples, enabling to assess conformity of unknown samples to EU legislation (REACH).

1. S. Radhakrishnan, H. Colaux, C. Vinod Chandran, D. Dom, L. Verheyden, F. Taulelle, J. Martens and E. Breynaert, *Anal. Chem.* 2020, **92**, 13004–13009.

**NMR crystallography reveals carbonate induced Al-ordering in ZnAl layered double hydroxide**

S. Radhakrishnan,<sup>1,2</sup> K. Lauwers,<sup>2</sup> C. Vinod Chandran,<sup>1,2</sup> J. Trébosc,<sup>3</sup> S. P. Sree,<sup>2</sup> J. A. Martens,<sup>1,2</sup> F. Taulelle,<sup>1,2</sup> C. E. A. Kirschhock<sup>2</sup> and E. Breynaert<sup>1,2</sup>

<sup>1</sup> NMRCoRe, KU Leuven

<sup>2</sup> Center for Surface Chemistry and Catalysis – Characterization and Application Team (COK-KAT), KU Leuven .

<sup>3</sup> Institut Michel-Eugène Chevreul, Univ. Lille, France

Layered double hydroxides (LDHs) serve a score of applications in catalysis, drug delivery, and environmental remediation. Smarter crystallography, combining X-ray diffraction and NMR spectroscopy revealed how interplay between carbonate and pH determines the LDH structure and Al ordering in ZnAl LDH. Carbonate intercalated ZnAl LDHs were synthesized at different pH (pH 8.5, pH 10.0, pH 12.5) with a Zn/Al ratio of 2, without subsequent hydrothermal treatment to avoid extensive recrystallisation. In ideal configuration, all Al cations should be part of the LDH and be coordinated with 6 Zn atoms, but NMR revealed two different Al local environments were present in all samples in a ratio dependent on synthesis pH. NMR-crystallography, integrating NMR spectroscopy and X-ray diffraction, succeeded to identify them as Al residing in the highly ordered crystalline phase, next to Al in disordered material. With increasing synthesis pH, crystallinity increased and the side phase fraction decreased. Using <sup>1</sup>H-<sup>13</sup>C, <sup>13</sup>C-<sup>27</sup>Al HETCOR NMR in combination with <sup>27</sup>Al MQMAS, <sup>27</sup>Al-DQ-SQ measurements and Rietveld refinement on high-resolution PXRD data, the extreme anion exchange selectivity of these LDHs for CO<sub>3</sub><sup>2-</sup> over HCO<sub>3</sub><sup>-</sup> was linked to strict Al and CO<sub>3</sub><sup>2-</sup> ordering in the crystalline LDH. Even upon equilibration of the LDH in pure NaHCO<sub>3</sub> solutions, only CO<sub>3</sub><sup>2-</sup> was adsorbed by the LDH. This reveals the structure directing role of bivalent cations such as CO<sub>3</sub><sup>2-</sup> during crystallisation of [M<sub>2+4</sub>M<sub>3+2</sub>(OH)<sub>2</sub>]<sub>2</sub>[A<sub>2-</sub>]<sub>1</sub>·yH<sub>2</sub>O LDH phases.

1. S. Radhakrishnan, K. Lauwers, C. Vinod Chandran, J. Trébosc, S. P. Sree, J. A. Martens, F. Taulelle, C. E. A. Kirschhock, E Breynaert, Chem. Eur. J. 2021, 27, 15944-15953.

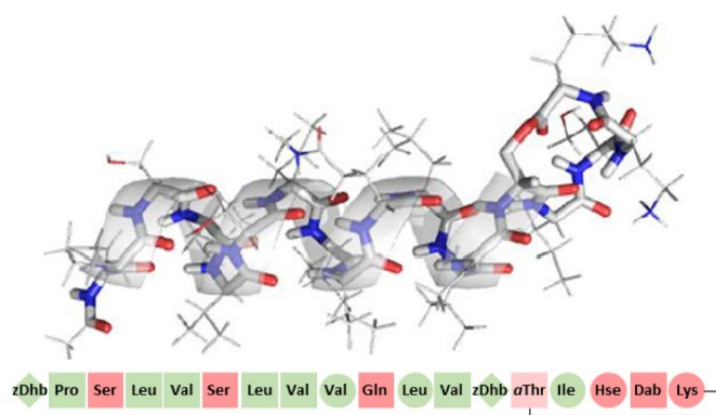
## P14

## The impact of macrocycle formation on the conformation of tolaasin I as revealed by NMR spectroscopy

D. Roelandt<sup>1</sup>, B. Kovács<sup>1</sup>, N. Geudens<sup>1</sup> and J.C. Martins<sup>1</sup>

<sup>1</sup> NMR & Structure Analysis Unit, Dept. of Organic and Macromolecular Chemistry, Ghent University, Ghent, Belgium

Cyclic lipopeptides (CLiPs) are a class of secondary metabolites that consist of a peptide moiety with an N-terminal lipid tail and a macrocycle formed via an ester bond (depsi) between the C-terminal carboxyl group and a side chain hydroxyl group. They are produced by multiple genera of bacteria including *Pseudomonas* and *Bacillus*. CLiPs exhibit a multitude of biological functions in Nature such as improving bacterial motility, antibacterial activity and antifungal activities among others. [1] More recent investigations by our group have also highlighted their antitumor activities.



Tolaasin, a CLiP produced by *Pseudomonas tolaasii*, is the causative agent for brown blotch disease in mushrooms. When tolaasin is released by the bacterium it forms pores in the membrane of epithelial mushroom cells, creating lesions which develop a brown colour, ruining the mushrooms for consumption. Recent studies have shown that a natural defence mechanism exists where the antagonistic properties of tolaasin are lost by hydrolysis of the depsi bond closing the macrocycle. This involves an

enzyme released by another bacterium inhabiting the same ecological niche. [2] Mainly unstructured in water, tolaasin adopts a stable amphipathic left handed  $\alpha$ -helix ending in a flattened macrocycle loop when exposed to micelle forming detergents such as SDS. [3] In this project we aim to better understand why loss of the macrocycle has such a marked effect on tolaasin activity by comparing the conformation adopted by hydrolysed tolaasin with that of the native molecule both studied in SDS micelles using NMR spectroscopy.

To allow the use of more elaborate multidimensional structure assignment and analysis methods, we first produced <sup>13</sup>C and <sup>15</sup>N isotope enriched tolaasin by growing the producing bacterium on minimal medium and suitable labelled isotopically enriched precursors. Next, we produced the isotopically enriched hydrolysed form by controlled alkaline hydrolysis followed by purification. Following full resonance assignment, HNHA measurements are first used to obtain the  $\phi$  torsion angle dependent <sup>3</sup>J<sub>HNHA</sub> coupling in both forms. Next, long range HNC0 measurements are recorded to identify the presence and location of long-lived hydrogen bonds through so called <sup>3</sup><sub>h</sub>J<sub>HN-C'</sub> scalar couplings. By comparing these coupling data in both tolaasin forms, changes in the conformation can be detected and interpreted. The experimental data will be complemented by Molecular Dynamics simulations of the interaction between the CLiP and the amphipathic SDS micellar surface in order to complete our understanding.

1. Geudens, N. and J.C. Martins, *Cyclic lipodepsipeptides from Pseudomonas spp.–biological swiss-army knives*. *Frontiers in microbiology*, 2018. **9**: p. 1867.
2. Hermenau, R., et al., *Helper bacteria halt and disarm mushroom pathogens by linearizing structurally diverse cyclolipopeptides*. *Proceedings of the National Academy of Sciences*, 2020. **117**(38): p. 23802-23806.
3. Jourdan, F., et al., *A left-handed  $\alpha$ -helix containing both L- and D-amino acids: The solution structure of the antimicrobial lipodepsipeptide tolaasin*. *Proteins: Structure, Function, and Bioinformatics*, 2003. **52**(4): p. 534-543.

**The non-innocent role of spin-traps in monitoring radical formation in copper-catalyzed reactions**

M. Samanipour<sup>1</sup>, H. Y. V. Ching<sup>1</sup>, H. Streckx<sup>2</sup>, B. U. W. Maes<sup>3</sup>, and S. Van Doorslaer<sup>1</sup>

1 Department of Chemistry, BIMEF, University of Antwerp, Antwerp, Belgium

2 Janssen Pharmaceutica, Janssen Pharmaceutica, Beerse, Belgium, Belgium.

3 Department of Chemistry, ORSY, University of Antwerp, Antwerp, Belgium

Spin-traps, like 5,5-dimethyl-1-pyrroline N-oxide (DMPO) are commonly used to identify radicals formed in numerous chemical and biological systems, many of which contain metal-ion complexes[1-3]. For example, in many of the copper-catalyzed synthesis pathways of organic molecules, the formation of highly reactive, short-living radical intermediates, such as reactive oxygen species (ROS, e.g. O<sub>2</sub>•-, •OH, ...) and carbon-centred radicals, are hypothesized to play a crucial role. Therefore spin-trap EPR has been abundantly used to support radical mechanisms in copper-catalyzed reactions, and very often the spin trap is added in very large excess, compared to the copper catalyst [3],[4]. Many studies have, however, pointed out considerable pitfalls in the use of spin-trap EPR, such as unwanted side reactions and follow-up reactions that may lead to serious misinterpretations. Despite the attention given to the potential pitfalls of spin-trap EPR in terms of radical formation, surprisingly little attention has been paid to the possibility that transition-metal ions may form a complex with the spin traps or that the spin traps can strongly alter the reaction mechanism under study. [4]

In this study, continuous-wave electron paramagnetic resonance and hyperfine spectroscopy are used to prove the equatorial ligation of DMPO(-derived) molecules to Cu(II), even in the presence of competing nitrogen bases. The experimental data are corroborated with density functional theory calculations. It is shown that <sup>14</sup>N HYSCORE can be used as a fingerprint method to reveal the coordination of DMPO(-derived) molecules to Cu(II), an interaction that might influence the outcome of spin-trapping experiments and consequently the conclusion drawn on the mechanism under study. [4]

1. Buettner, G. R. *Free Radical Biology and Medicine*.1987, 3(4), 259-303.

2. Alberti, A. and Macciantelli, D., In *Electron Paramagnetic Resonance – A Practitioner's Toolkit*, 2009, 287.

3. Hawkins, C. L., Davies, M. J., *Biochim. Biophys. Acta* 2014 1840, 708.

4. Samanipour, M., Ching, H. Y. V., Streckx, H., Maes, B. U. W., and Van Doorslaer, S., *Appl Magn Reson*. 2020, 51, 1529-1542

## Towards a better understanding of the underlying molecular mechanisms during an aptamer-target interaction, an NMR analysis of TESS.1

S. Schellinck<sup>1</sup>, A.M. de Vries<sup>1,2</sup>, D. Buyst<sup>3</sup>, E. Daems<sup>4,5,6</sup>, R. Cánovas<sup>4,5</sup>, K. De Wael<sup>4,5</sup>, A.Madder<sup>2</sup>, J.C. Martins<sup>1</sup>

<sup>1</sup> NMR and Structure Analysis Research Group, Department of Organic and Macromolecular Chemistry, Ghent University, Ghent 9000, Belgium.

<sup>2</sup> Organic and Biomimetic Chemistry Research Group, Department of Organic and Macromolecular Chemistry, Ghent University, Ghent 9000, Belgium.

<sup>3</sup> Department of Organic and Macromolecular Chemistry, NMR Centre of Expertise, Ghent University, Ghent, Oost-Vlaanderen, 9000, Belgium

<sup>4</sup> A-Sense Lab, Department of Bioscience Engineering, University of Antwerp, Groenenborgerlaan 171, 2020 Antwerp, Belgium.

<sup>4</sup> NANOLab Center of Excellence, University of Antwerp, Groenenborgerlaan 171, 2020 Antwerp, Belgium.

<sup>5</sup> BAMS Research Group, Department of Chemistry, University of Antwerp, Groenenborgerlaan 171, 2020 Antwerp, Belgium.

Steroid hormones regulate many physiological processes, for example those of the reproductive system. Because of their importance in medical research and diagnosis, studies towards more efficient, selective detection and real-time monitoring at low concentrations are in high demand. This need has resulted in the development of so called ‘aptasensors’. The biological component in these biosensors are aptamers, short single stranded oligonucleotides raised to bind a certain predefined target with high affinity, in this case a steroid hormone. The proposed working mechanism of aptasensors is based on detecting a change in a particular signal (fluorescence, electric current,...) as a result of the conformational change of the aptamer upon binding with its target. Although simple and convincing in design, not much is actually known about the underlying molecular mechanisms taking place during such an aptamer-target interaction and the way in which the conformation of the aptamer changes.

NMR spectroscopy is in principle well suited to study conformational changes and intermolecular interactions [2]. To explore if NMR could provide insight into the molecular events occurring in aptamer based biosensors, we chose the testosterone binding TESS.1 aptamer as a well described model system for investigation [1]. We first devised a titration protocol which handles the challenge posed by the limited solubility of testosterone in aqueous media (~80 µM). By monitoring the NMR signals of the aptamer and target during titration studies marked conformational changes are indeed detected. However, the large size of the oligonucleotide sequence precludes assignment and further investigation. We will show that by trimming the duplex stem of the aptamer and by introducing some nucleotide substitutions, a more ‘NMR optimal’ sequence is obtained that still interacts with testosterone in a fashion similar to the original sequence. The reduced size and modifications generate simplified NMR spectra allowing better analysis and interpretation of the aptamer-target interaction.

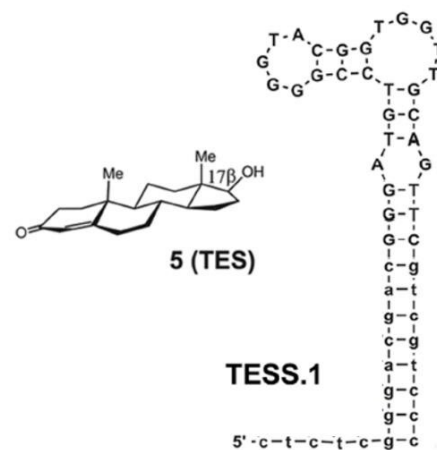


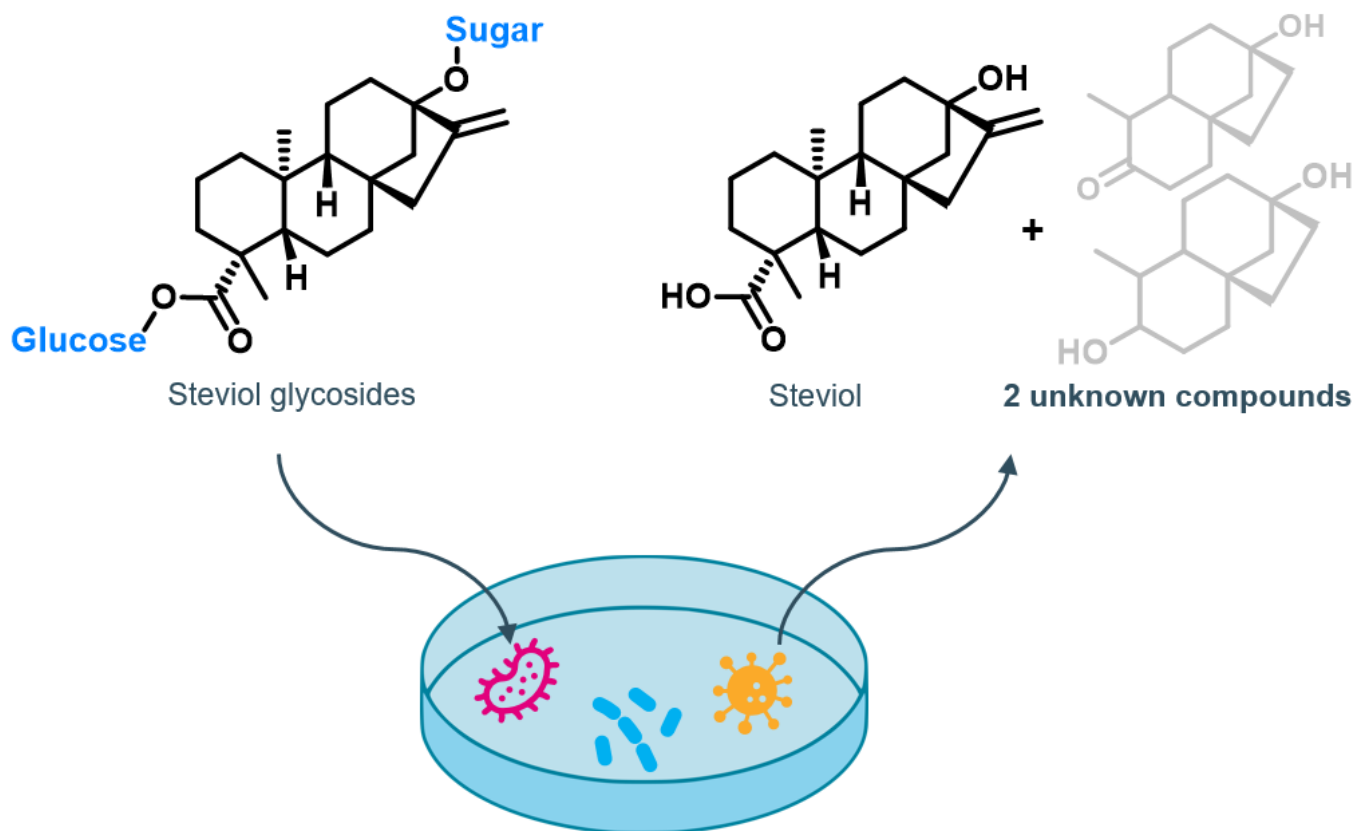
Figure 1: Sequence of the TESS.1 aptamer and structure of the steroid testosterone (adapted from [1])

1. Yang, K.A., et al., *High-Affinity Nucleic-Acid-Based Receptors for Steroids*. *Acs Chemical Biology*, 2017. **12**(12): p. 3103-3112.

2. Roberts, G.C.K., ed., *NMR of macromolecules: a practical approach*. The Practical Approach Series, ed. B.D.H. D. Rickwood. Vol. 134. 1993: Oxford University Press: Oxford.

**Characterization of Microbial Degradation Products of Steviol Glycosides**G. Steurs<sup>1</sup>, N. Moons<sup>1</sup>, L. Van Meervelt<sup>2</sup>, B. Meesschaert<sup>3</sup> and W. M. De Borggraeve<sup>1</sup><sup>1</sup> Division of Molecular Design and Synthesis, Department of Chemistry, KU Leuven, Leuven.<sup>2</sup> Division of Biochemistry, Molecular and Structural Biology, Department of Chemistry, KU Leuven, Leuven.<sup>3</sup> Laboratory for Microbial and Biochemical Technology, Department of Microbial and Molecular Systems, KU Leuven Bruges Campus, Bruges.

Steviol glycosides were subjected to bacteria present in a soil sample collected from a Stevia plantation in Paraguay. During the incubation experiments, next to the aglycon steviol, steviol degradation products were also formed. X-ray analysis and NMR methods in combination with chemical synthesis and GIAO NMR calculations were used to fully characterize the structure of these compounds as a tricyclic ketone and the corresponding reduced form. They were nicknamed *monicanone* and *monicanol*. The latter has the (S)-configuration at the alcohol site.<sup>1</sup>

**Graphical abstract**

1. Steurs, G.; Moons, N.; Van Meervelt, L.; Meesschaert, B.; De Borggraeve, W. M., Characterization of Microbial Degradation Products of Steviol Glycosides. *Molecules* **2021**, 26 (22), 6916.

**Isotopological Fingerprinting Enables Conformational Analysis of Hydrogenation Catalysts**

E. Vaneckhaute<sup>1</sup>, J.-M. Tyburn<sup>2</sup>, J. G. Kempf<sup>3</sup>, J. A. Martens<sup>1</sup> and E. Breynaert<sup>1</sup>

<sup>1</sup>NMRCoRe, COK-KAT, KULeuven

<sup>2</sup>Bruker Biospin, Germany

<sup>3</sup>Bruker Biospin, United States

Parahydrogen (p-H<sub>2</sub>) induced hyperpolarization requires symmetry breaking of p-H<sub>2</sub> to convert singlet spin order into observable enhanced magnetization.<sup>1</sup> Signal amplification by reversible exchange (SABRE) applies reversible transition metal complexation of both p-H<sub>2</sub> and target molecules to induce a temporary symmetry breaking event for transfer of polarization. At high magnetic field singlet-triplet mixing governed by chemically inequivalent hydride positions can spontaneously generate non-thermal longitudinal two-spin order that can be used for catalyst conformational analysis.<sup>2</sup>

Here we present a method for rigorous stereo-conformational investigation of iridium complexation in presence of various ligands in an exchangeable solvent. Simple addition of protons in a fully deuterated environment (CD<sub>3</sub>OD) acts as an alternative 'labelling' technique for N-containing ligands. Depending on their functionality different isotopologues (-NH<sub>x</sub>D<sub>y</sub>) are generated and variations in trans-hydride chemical shift become apparent.

Hyperpolarized 2D Zero-Quantum Coherence NMR is then employed to visualize these isotopological variations, in less than 1 minute. Here the long-lasting longitudinal two-spin order discriminates the hydride couples after excitation by evolving under the chemical shift difference between them. This provides exciting opportunities to rapidly distinguish multiple binding sites on transition metals and identify all active hydride complexes.

1 Bowers, C.R. & Weitekamp, D.P. *J. Am. Chem. Soc.* **109**, 5541–5542.

2 Eshuis, N. et al. *Angew. Chemie - Int. Ed.* **54**, 14527–14530.



**P19****Quantification of 2-disulfide bonded isomers of apamin, a peptidic toxin, leads to the observation of a structural rearrangement**

M. Wanko<sup>1</sup>, J.L. Hayen<sup>3</sup>, R. Vitello<sup>2</sup>, C. Damblon<sup>1</sup>, J.F. Liégeois<sup>2</sup>

*1 Division MoISys, Université de Liège, Liège*

*2 Division CIRM, Université de Liège, Liège*

*3 Université de Liège, Liège*

Apamin is an octadecapeptide with four cysteine residues assembled in two disulfide bridges. The compound interacts strongly with SK channels and blocks corresponding SK currents. In the context of our program related to the development of blockers of SK channels, we were interested in assessing the biological activity of two isomers of apamin. These peptides present another disulfide bond connectivity. These peptides were produced by chemical synthesis.

Before these biological evaluations, the quantification of peptide content in our samples was needed.

After the quantification, we observed in both solutions of isomers a change in the composition.



## LIST OF PARTICIPANTS

<b>Aprile</b>	Carmela	UNamur	carmel.aprile@unamur.be
<b>Abdelhameed</b>	Shorok	KU Leuven	shorok.abdelhameed@kuleuven.be
<b>Adriaensens</b>	Peter	UHasselt	peter.adriaensens@uhasselt.be
<b>Banci</b>	Lucia	UniFI	lucia.banci@unifi.it
<b>Barozzino</b>	Gabriella	UCLouvain	gabriella.barozzino@uclouvain.be
<b>Bernardi</b>	Marie	UMons	marie.bernardi@umons.ac.be
<b>Bondeville</b>	Victoire	UCLouvain	victoire.bondeville@student.uclouvain.be
<b>Bruylants</b>	Gilles	ULB	gilles.bruylants@ulb.be
<b>Buyse</b>	Chloe	UCLouvain	chloe.buyse@uclouvain.be
<b>Buyst</b>	Dieter	UGent	dieter.buyst@ugent.be
<b>Célis</b>	Chloé	UNamur	chloe.celis@unamur.be
<b>Callewaert</b>	Bram	KU Leuven	bram.callewaert@kuleuven.be
<b>Cataldo</b>	Alessio	ULB	alessio.cataldo@ulb.be
<b>Chandrasekharan</b>	Vinodchandran	KU Leuven	vinod@kuleuven.be
<b>Ching</b>	Vincent	UAntwerpen	hongyuevincent.ching@uantwerpen.be
<b>Ciobanu</b>	Luisa	CEA Saclay	luisa.ciobanu@cea.fr
<b>Claes</b>	Hannes	KU Leuven	hannes.claes1@kuleuven.be
<b>Conq</b>	Jérôme	UCLouvain	jerome.conq@uclouvain.be
<b>Cools</b>	Lennert	KU Leuven	lennert.cools@kuleuven.com
<b>Damblon</b>	Christian	ULiège	c.damblon@uliege.be
<b>De Borggraeve</b>	Wim	KU Leuven	wim.deborggraeve@kuleuven.be
<b>De Leener</b>	Gaël	ULB	gael58@gmail.com
<b>de Oliveira Silva</b>	Rodrigo	KU Leuven	rodrigo.deoliveirasilva@kuleuven.be
<b>De Ruyscher</b>	Dries	VIB-KU Leuven	dries.deruyscher@kuleuven.be
<b>Derveaux</b>	Elien	UHasselt	elien.derveaux@uhasselt.be
<b>d'Hose</b>	Donatienne	UCLouvain	donatienne.dhose@uclouvain.be
<b>Emsley</b>	Lyndon	EPFL	lyndon.emsley@epfl.ch
<b>Ernotte</b>	Pierre	UMons	pierre.ernotte@umons.ac.be
<b>Farah</b>	Chantale	UCLouvain	chantale.farah@uclouvain.be
<b>Freichels</b>	Hélène	Magritek	helene@magritek.com
<b>Fusaro</b>	Luca	UNamur	luca.fusaro@unamur.be
<b>Gallez</b>	Bernard	UCLouvain	bernard.gallez@uclouvain.be
<b>Geudens</b>	Niels	UGent	niels.geudens@ugent.be
<b>Gosee</b>	Camille	UMons	camille.gosee@umons.ac.be
<b>Gossuin</b>	Yves	UMONS	yves.gossuin@umons.ac.be
<b>Guidetti</b>	Andrea	UAntwerpen	Andrea.Guidetti@uantwerpen.be
<b>Gys</b>	Nick	VITO	nick.gys@vito.be
<b>Henoumont</b>	Céline	UMons	celine.henoumont@umons.ac.be
<b>Himmelreich</b>	Uwe	KU Leuven	uwe.himmelreich@kuleuven.be
<b>Jordan</b>	Benedicte	UCLouvain	benedicte.jordan@uclouvain.be
<b>Joudiou</b>	Nicolas	UCLouvain	nicolas.joudiou@uclouvain.be
<b>Khan</b>	Nasar	KU Leuven	nasar.khan@kuleuven.be
<b>Laurent</b>	Sophie	UMons	sophie.laurent@umons.ac.be
<b>Lepicard</b>	Elise	UCLouvain	elise.lepicard@uclouvain.be
<b>Lesclinier</b>	Eveline	KU Leuven	eveline.lesclinier@kuleuven.be
<b>Maertens</b>	Amélie	UNamur	amelie.maertens@unamur.be
<b>Martin</b>	Éléonore	UMons	eleonore.martin@umons.ac.be

<b>Martins</b>	Jose	UGent	Jose.Martins@UGent.be
<b>Mathieu</b>	Barbara	UCLouvain	barbara.mathieu@uclouvain.be
<b>Mignion</b>	Lionel	UCLouvain	lionel.mignion@uclouvain.be
<b>Morena</b>	Anthony	UNamur	anthony.morena@unamur.be
<b>Moussawi</b>	Mhamad Aly	KU Leuven	mhamadaly.moussawi@kuleuven.be
<b>Natacha</b>	Dehaen	UCLouvain	natacha.dehaen@uclouvain.be
<b>Olla</b>	Chiara	UNamur	chiara.olla@dsf.unica.it
<b>Parac-Vogt</b>	Tatjana	KU Leuven	tatjana.vogt@kuleuven.be
<b>Penders</b>	Marc	Bruker	marc.penders@bruker.com
<b>Prisner</b>	Thomas	Goethe University	prisner@chemie.uni-frankfurt.de
<b>Pusovnik</b>	Matic	KU Leuven	matic.pusovnik@kuleuven.be
<b>Radhakrishnan</b>	Sambhu	KU Leuven	sambhu.radhakrishnan@kuleuven.be
<b>Reekmans</b>	Gunter	UHasselt	gunter.reekmans@uhasselt.be
<b>Roelandt</b>	Dries	UGent	dries.roelandt@ugent.be
<b>Sabine Van Doorslaer</b>	Sabine	UAntwerpen	sabine.vandoorslaer@uantwerpen.be
<b>Sakellariou</b>	Dimitrios	KU Leuven	dimitrios.sakellariou@kuleuven.be
<b>Salazar Marcano</b>	David	KU Leuven	david.salazarmarcano@kuleuven.be
<b>Samanipour</b>	Mohammad	UAntwerpen	m.samanipoor66@gmail.com
<b>Schellinck</b>	Sofie	UGent	sofie.schellinck@ugent.be
<b>Serra</b>	Ilenia	UAntwerpen	Ilenia.Serra@uantwerpen.be
<b>Soumoy</b>	Lorraine	UNamur	loraine.soumoy@unamur.be
<b>Stanicki</b>	Dimitri	UMons	dimitri.stanicki@umons.ac.be
<b>Stefanoska</b>	Lidija	ULB	Lidija.Stefanoska@ulb.be
<b>Steurs</b>	Gert	KU Leuven	gert.steurs@kuleuven.be
<b>Swinnen</b>	Siene	KU Leuven	siene.swinnen@kuleuven.be
<b>Valentino</b>	Laura	UNamur	laura.valentino@unamur.be
<b>Van den Bergh</b>	Lore	UAntwerpen	lore.vandenbergh@uantwerpen.be
<b>Van Gompel</b>	Wouter	UHasselt	wouter.vangompel@uhasselt.be
<b>Van Lommel</b>	Ruben	KU Leuven	ruben.vanlommel@kuleuven.be
<b>Vanduffel</b>	An	KU Leuven	anvanduffel@hotmail.com
<b>Vanduffel</b>	Hanne	KU Leuven	hanne.vanduffel@kuleuven.be
<b>Vaneeckhaute</b>	Ewoud	KU Leuven	ewoud.vaneeckhaute@kuleuven.be
<b>Vivian</b>	Alvise	UNamur	alvise.vivian@unamur.be
<b>Wanko</b>	Marius	ULiège	amwanko@uliege.be
<b>Weckx</b>	Pasquinel	KU Leuven	pasquinel.weckx@kuleuven.be
<b>Wehbi</b>	Mohammad	UCLouvain	mohammadwehbi1889@outlook.com
<b>Wong</b>	Chu	Bruker	Chu.Wong@bruker.com
<b>Yelek</b>	Caner	UCLouvain	caner.yelek@uclouvain.be
<b>Yu</b>	Ziyou	KU Leuven	ziyou.yu@kuleuven.be